Development 139, 1921-1930 (2012) doi:10.1242/dev.078543

The regenerative capacity of the zebrafish heart is dependent on TGFβ signaling

Fabian Chablais* and Anna Jaźwińska*,‡

SUMMARY

Mammals respond to a myocardial infarction by irreversible scar formation. By contrast, zebrafish are able to resolve the scar and to regenerate functional cardiac muscle. It is not known how opposing cellular responses of fibrosis and new myocardium formation are spatially and temporally coordinated during heart regeneration in zebrafish. Here, we report that the balance between the reparative and regenerative processes is achieved through Smad3-dependent TGFβ signaling. The type I receptor *alk5b* (*tgfbr1b*) is expressed in both fibrotic and cardiac cells of the injured heart. TGFβ ligands are locally induced following cryoinjury and activate the signaling pathway both in the infarct area and in cardiomyocytes in the vicinity of the trauma zone. Inhibition of the relevant type I receptors with the specific chemical inhibitor SB431542 qualitatively altered the infarct tissue and completely abolished heart regeneration. We show that transient scar formation is an essential step to maintain robustness of the damaged ventricular wall prior to cardiomyocyte replacement. Taking advantage of the reversible action of the inhibitor, we dissected the multifunctional role of TGFβ signaling into three crucial processes: collagen-rich scar deposition, Tenascin C-associated tissue remodeling at the infarct-myocardium interface, and cardiomyocyte proliferation. Thus, TGFβ signaling orchestrates the beneficial interplay between scar-based repair and cardiomyocyte-based regeneration to achieve complete heart regeneration.

KEY WORDS: Cryoinjury, Heart regeneration, TGFβ, Zebrafish

INTRODUCTION

In adult mammals, a heart infarction heals by deposition of a permanent collagenous scar instead of restoration of functional cardiac tissue (Laflamme and Murry, 2011). By contrast, an impressive regenerative capacity has been demonstrated in the heart of zebrafish and newts (Ausoni and Sartore, 2009; Major and Poss, 2007; Singh et al., 2010). In contrast to mammals, these animals sustain a robust proliferative competence of cardiomyocytes in adult life, which provides a source of a new myocardium.

The zebrafish serves as a particularly useful model system with which to study the regenerative response to myocardial damage, as shown by experiments involving resection of the ventricular apex, cryoinjury and genetic cardiomyocyte depletion (Chablais et al., 2011; Gonzalez-Rosa et al., 2011; Schnabel et al., 2011; Wang et al., 2011). Cell lineage-tracing analyses have demonstrated that complete repair of the amputated myocardial apex predominantly involves cell cycle re-entry of existing cardiomyocytes, as opposed to recruitment of epicardial stem cells (Jopling et al., 2010; Kikuchi et al., 2011a; Kikuchi et al., 2010). Despite progress in the last decade, little is known about the molecular factors that control heart restoration. Studies applying transgenesis have revealed a requirement of the FGF and retinoic acid (RA) signaling pathways in epicardial activation and in stimulation of cardiomyocyte proliferation (Kikuchi et al., 2011b; Lepilina et al., 2006). Using a small-molecule inhibition approach it has been shown that PDGF signaling is required for epicardial function and blood vessel formation in regenerating zebrafish hearts (Kim et al., 2010; Lien et al., 2006). These findings support the hypothesis that organ regeneration is regulated by secreted factors that mediate communication between adjacent cardiac and non-cardiac tissues.

The advantage of the zebrafish model system in regenerative biology has recently been reinforced by establishing a myocardial infarction model using a cryoinjury procedure, which involves direct freezing of the ventricular wall (Chablais et al., 2011; Gonzalez-Rosa et al., 2011; Schnabel et al., 2011). Compared with ventricular resection or genetic cardiomyocyte depletion, this procedure is of particular value because it mimics different physiological responses observed in mammals, including cell death and scarring. After reparative events, zebrafish infarcted hearts progress to a unique regenerative phase. The initially deposited scar tissue becomes completely replaced with new cardiac muscle within 2 months following cryoinjury. Remarkably, proliferation of cardiomyocytes is triggered simultaneously with the scar deposition. The progressive cardiomyocyte propagation into the injury area is accompanied by local regression of fibrotic tissue. Thus, cardiac regeneration involves different responses of cardiac and non-cardiac cell types, which have to be spatially and temporally orchestrated to achieve a balance between the reparative and regenerative processes. Little is known about the molecules that coordinate the function of the various cellular components to achieve this successful regeneration.

In the present study, we identified that a molecular link between the reparative and regenerative processes after cryoinjury-induced myocardial infarction is achieved through Smad3-dependent TGFβ/Activin signaling. We first determined the involvement of the related TGFβ and Activin-β (Inhibin β) ligands using expression analysis at the transcript and protein levels. Next, we visualized the spatiotemporal dynamics of pathway activation during heart regeneration using immunostaining of a direct

Unit of Anatomy, Department of Medicine, University of Fribourg, Rte A. Gockel 1, 1700 Fribourg, Switzerland.

*Present address: Department of Biology, University of Fribourg, Ch. du Musée 10, 1700 Fribourg, Switzerland
‡Author for correspondence (anna.jazwinska@unifr.ch)

Accepted 19 March 2012

downstream signal transducer, phospho-Smad3. To determine the role of TGFβ/Activin signaling, we blocked the relevant type I receptor with the previously characterized specific inhibitor SB431542. Inhibition of TGFβ/Activin signaling suppressed phosphorylation of Smad3 and impaired heart regeneration, resulting in ventricular deformation. The reversible action of the inhibitor was beneficial in dissecting the effects of TGFβ signaling on several successive cellular processes. The temporal inhibition of TGFβ/Activin signaling during the subacute phase revealed an unexpected role of the transient scar in supporting the mechanical properties of the damaged ventricle. We identified several extracellular regulators of tissue organization and remodeling, represented by Collagen, Fibronectin and Tenascin C, as targets of TGFβ/Activin signaling. Furthermore, continuous and short-term inhibition of the pathway demonstrated the stimulatory role of TGFβ/Activins for cardiomyocyte proliferation, which is a key mechanism of new myocardium formation. Our study provides evidence that TGFβ signaling coordinates a wide spectrum of subsequent cellular steps that are required for efficient heart regeneration in zebrafish.

MATERIALS AND METHODS

Animal procedures

The following zebrafish strains were used: wild-type AB (Oregon), *cmlc2::DsRed2-Nuc* (Rottbauer et al., 2002), *flk1::EGFP* (Lawson and Weinstein, 2002) and *hsp70:dn-fgfr1* (Lepilina et al., 2006). Fish at 6-18 months of age were anesthetized in 0.1% tricaine (Sigma-Aldrich) and cryoinjury was performed as previously described (Chablais et al., 2011). Ventricular apex resection was performed as described (Poss et al., 2002). Animals were allowed to regenerate for various times at 26.5°C. The Alk5/4 inhibitor SB431542 (Tocris) was used as previously described (Jazwinska et al., 2007). The control fish were in water with 0.1% DMSO. For BrdU incorporation analysis, the fish were incubated for 24 hours in water containing 50 μg/ml BrdU (Sigma-Aldrich). *hsp70:dn-fgfr1* fish received daily heat shocks by raising the water temperature to 37°C for 1 hour. The experimental research on animals was approved by the cantonal veterinary office of Fribourg.

Histological techniques and immunohistochemistry

Acid Fuchsin Orange-G (AFOG) staining was performed as described previously (Poss et al., 2002). For immunohistochemistry, the primary antibodies used were: rabbit anti-TGFβ receptor I at 1:50 (AnaSpec, 53895), mouse anti-Tropomyosin at 1:100 [developed by Jung-Ching Lin, obtained from the Developmental Studies Hybridoma Bank (DSHB), CH1], mouse anti-GFP at 1:100 (Roche, 11814460001), rabbit anti-Raldh2 at 1:400 (GeneTex, GTX124302), rabbit anti-Tenascin C at 1:500 (USBiological, T2550-23), mouse anti-Vimentin at 1:70 (developed by Alvarez-Buylla, obtained from DSHB, 40E-C), rabbit anti-α-SMA at 1:200 (GeneTex, GTX1000345), rabbit anti-Mcm5 at 1:5000 (kindly provided by Soojin Ryu, MPI for Medical Research, Heidelberg, Germany), rabbit anti-Fibronectin at 1:400 (Sigma-Aldrich, F3648), rabbit anti-phospho-Smad3 at 1:400 (Abcam, ab52903) and rat anti-BrdU at 1:100 (Abcam, ab6326). The secondary antibodies used (at 1:500) were: goat anti-rabbit Alexa Fluor 488, goat anti-mouse Alexa Fluor 488 (Molecular Probes), goat anti-rabbit Cy3 or Cy5 conjugated, goat anti-mouse DyLight 549 or 649 conjugated (Jackson ImmunoResearch).

Hearts were fixed, cryosectioned at 16 μm and immunostained as previously described (Chablais et al., 2011). The specimens were analyzed by confocal microscopy (Leica TCS-SP5). For quantification of proliferating cardiac cells, Mcm5/DsRed2 or BrdU/DsRed2 double-positive nuclei were normalized as the percentage of the total number of DsRed2-positive nuclei using ImageJ 1.44p software. For quantification of proliferating non-cardiac cells, the number of Mcm5-positive DsRed-negative cells was normalized as the percentage of the total number of DAPI-positive cells of the ventricle.

In situ hybridization

In situ hybridization on cryosections was performed as described (Chablais and Jazwinska, 2010). Primers are listed in supplementary material Table S1.

In situ hybridization combined with antibody staining

After standard in situ hybridization staining, the sections were washed in PBS for 30 minutes and postfixed in 70% ethanol for 30 minutes. The slides were rinsed in PBST (PBS, 0.3% Triton X-100) and incubated with PBST plus 5% goat serum for 1 hour. The primary antibodies are listed above. The slides were processed using the Vectastain ABC Kit (Vector Labs) according to the manufacturer's instructions. Secondary antibodies (Vector Labs) were biotinylated anti-mouse (BA-2000) and biotinylated anti-rabbit (BA-1000) diluted 1:200. The antibody staining was detected using DAB solution (Sigma-Aldrich, D5905).

Electrocardiogram (ECG) recordings and acquisition

All ECGs were recorded in triplicate before injury and at subsequent time points after surgery. To reduce biological variation, the same six animals were recorded before and after injury. ECG acquisitions were performed as previously described (Chablais et al., 2011).

RESULTS

Induction of TGFβ signaling in the regenerating zebrafish heart

A class of molecular signals that are known to be injury activated in various organs is represented by structurally related TGFβ and Activin cytokines (Dobaczewski et al., 2010a; Werner and Alzheimer, 2006). In vertebrates, several isoforms of these family members have been identified (Massague and Gomis, 2006). We tested the expression of Activin and TGFβ genes by in situ hybridization using control hearts from sham-injured zebrafish [4 days post sham (dps)] and regenerating hearts at the onset of infarct healing [4 days post cryoinjury (dpci)], and at 14 dpci when the transition between scar formation and scar resorption becomes evident. *activin-βA* (*inhbaa* – Zebrafish Information Network) was not significantly detected in control and injured hearts, whereas *activin-βB* (*inhbb* – Zebrafish Information Network) was ubiquitously expressed only in regenerating hearts (supplementary material Fig. S1). By contrast, three known TGFβ isoforms, *tgfb1*, *tgfb2* and *tgfb3*, showed specific upregulation in the post-infarct zone of the injured hearts at 4 and 14 dpci (Fig. 1F-H and supplementary material Fig. S2A-D). The injury area was identified by the absence of the *ventricular myosin heavy chain* (*vmhc*) transcript (Fig. 1E). The control hearts did express TGFβ genes (Fig. 1A-D).

To further determine the expression domain of the TGFβ isoforms in the infarcted hearts, we combined in situ hybridization with antibody staining for marker proteins of different cell types in the heart. High-resolution imaging of double-stained sections did not reveal expression of TGFβ genes in the intact Tropomyosin-positive myocardium, except for a thin layer of cardiomyocytes abutting the infarct area (Fig. 1I and supplementary material Fig. S2H,I). Most of the Raldh2-expressing epicardial cells and Vimentin-expressing fibroblasts of the post-infarct appeared to be positive for the TGFβ transcripts (Fig. 1J,K and supplementary material Fig. S2J-M). By contrast, EGFP-labeled endothelial cells did not seem to display TGFβ expression (Fig. 1L and supplementary material Fig. S2N,O). We concluded that all three TGFβ genes appear to be expressed in overlapping domains that encompass several cell types, including fibroblasts and epithelial cells of the infarct area, as well as some cardiomyocytes at the infarct boundary.

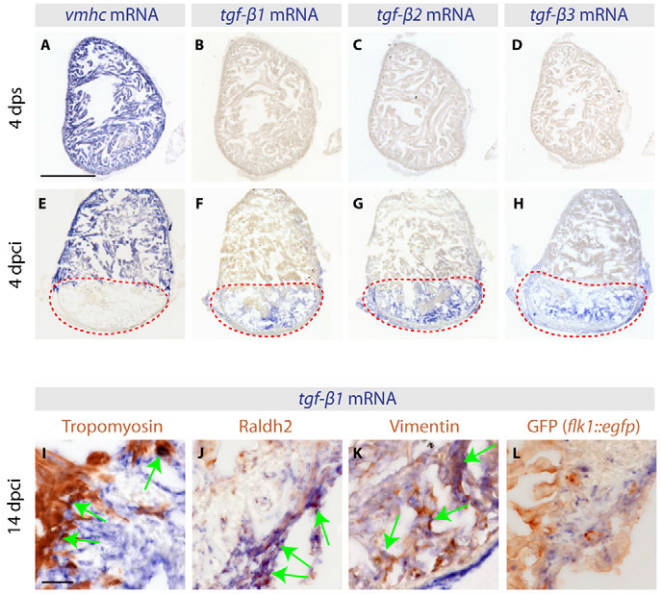

Fig. 1. Three TGFβ ligands are expressed in the infarct zone following cryoinjury. (**A-H**) In situ hybridization of consecutive heart sections with *vmhc*, *tgfb1*, *tgfb2* and *tgfb3* mRNA antisense probes (blue) of control zebrafish hearts at 4 days post sham surgery (dps) (A-D) and of cryoinjured hearts at 4 days post cryoinjury (dpci) (E-H). Red dashed lines encircle the injured areas. (A,E) At 4 dps, *vmhc* expression labels the intact ventricle. (B-D) None of the three TGFβ transcripts is detected in uninjured hearts. (E) The absence of *vmhc* mRNA demarcates the infarct area at 4 dpci. (F-H) At 4 dpci, *tgfb1*, *tgfb2* and *tgfb3* are upregulated in the injured area. (**I-L**) Heart sections at 14 dpci double-stained by in situ hybridization using *tgfb1* probe (blue) and immunohistochemistry using different cell type markers (brown). Arrows indicate double-positive cells. (I) Intact Tropomyosin-labeled myocardium does not express *tgfb1*, with the exception of cardiomyocytes abutting the infarct. (J) Raldh2-positive epicardial cells invading the injury area are co-labeled by *tgfb1* staining. (K) Vimentin-expressing fibroblasts of the infarct express *tgfb1*. (L) GFP expressed under the endothelial cell promoter *flk1* (*kdrl* – Zebrafish Information Network) does not colocalize with *tgfb1*. Scale bars: 300 μm in A; 50 μm in I.

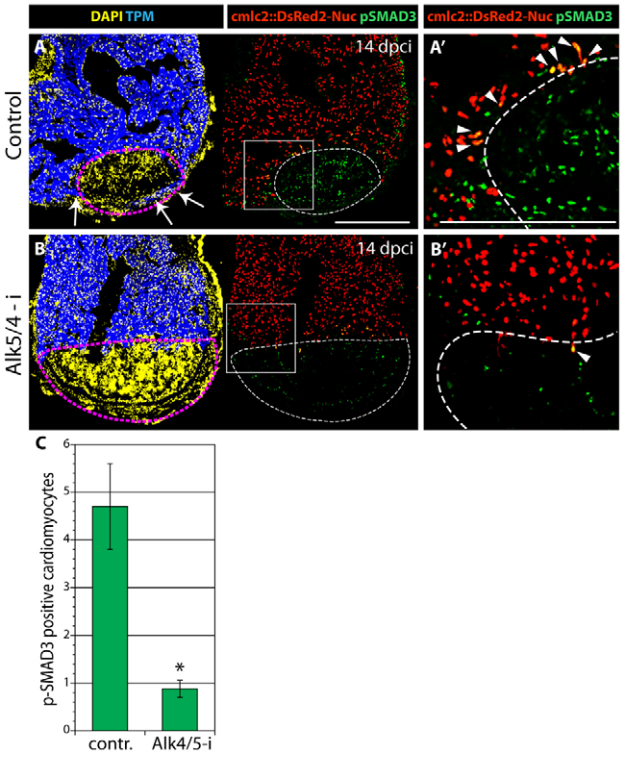

Fig. 2. Smad3-dependent TGFβ/Activin signaling is suppressed by the SB431542 inhibitor (Alk5/4-i) after myocardial infarction. (**A-B′**) At 14 dpci, heart sections from transgenic fish expressing nuclear DsRed2 (red) under the *cmlc2* cardiomyocyte-specific promoter were immunoassayed for Tropomyosin (TPM, blue) to visualize the intact myocardium and phospho-Smad3 (pSmad3, green). DAPI (yellow in the left panels) marks all the nuclei. The infarct is determined by the absence of Tropomyosin and DsRed2 expression (encircled by dashed lines). (A′,B′) Higher magnifications of the boxed areas in A,B. pSmad3-positive cardiomyocytes are indicated with arrowheads. (A,A′) Control regenerating hearts display numerous pSmad3-positive nuclei (green) in the injury area and in some cardiomyocytes at the infarct boundary. Arrows (A) indicate new myocardium surrounding the post-infarct. (B,B′) Treatment with 10 μM Alk5/4-i severely reduces pSmad3 staining. The injury area is larger than in the control and no invasion of cardiomyocytes is detected. (**C**) Quantification of pSmad3-positive cardiomyocytes in control and Alk5/4-i-treated hearts at 14 dpci. Error bars indicate s.e.m.; n=9; *P<0.01, t-test. Scale bars: 300 μm.

The TGFβ/Activin cytokines activate the downstream pathway via ligand-stimulated interaction of type I and II receptors (Massague and Gomis, 2006). We analyzed the expression of three isoforms of type I receptors, *alk5a/b* and *alk4* (*tgfbr1a/b* and *acvr1b* – Zebrafish Information Network), which are specific for TGFβs and Activins, respectively (Shi and Massague, 2003). *alk5a* and *alk4* appeared to be present in the injured area, whereas *alk5b* was strongly expressed in the entire heart (supplementary material Fig. S3). To confirm this finding, we visualized the distribution of Alk5b protein using an antibody against a unique amino acid sequence of this receptor. Immunofluorescence analysis detected the presence of this transmembrane receptor in the whole heart, including cardiomyocytes and Vimentin-positive cells of the post-infarct (supplementary material Figs S4 and S5). We concluded that both cardiac and non-cardiac cells of the infarcted heart can be responsive to TGFβ ligands.

The activated type I receptors transmit signaling by phosphorylation of receptor-activated SMADs (R-SMADs), which, in a complex with common-mediator SMADs (co-SMADs), are translocated to the nucleus to control target gene transcription (Shi and Massague, 2003). To determine the spatiotemporal activation of the TGFβ/Activin signaling pathway during cardiac regeneration, we visualized phospho-Smad3 (pSmad3), a specific R-SMAD for Alk5/4 receptors. To distinguish between cardiac and non-cardiac nuclei, we used a transgenic strain of zebrafish that expresses nuclear DsRed2 under the control of the cardiac-specific *cardiac myosin light chain* (*cmlc2*; *myl7* – Zebrafish Information Network) promoter (*cmlc2::DsRed2-Nuc*) (Rottbauer et al., 2002). To recognize healthy myocardium, the sections were immunostained for Tropomyosin. In hearts of uninjured fish, we did not detect significant pSmad3 immunolabeling (supplementary material Fig. S6A). However, the hearts at 7 and 14 dpci displayed numerous pSmad3-positive nuclei of non-cardiac cells in the post-infarct (Fig. 2A and supplementary

material Fig. S6B). Importantly, pSmad3 was also enhanced in a subset of cardiomyocytes localized at the infarct boundary (Fig. 2A). The number of pSmad3-positive nuclei declined at 30 dpci, when cardiac regeneration was nearly complete (supplementary material Fig. S6C,D). The visualization of pSmad3 demonstrates that the TGFβ/Activin signaling pathway is activated in the fibrotic tissue and in adjacent cardiomyocytes during heart restoration.

A small-molecule inhibitor of TGFβ receptor type I blocks heart regeneration resulting in a bulging infarct phenotype

To examine the requirement of the TGFβ/Activin pathway for heart regeneration, we applied a pharmacological strategy to block type I receptor activity. We used the low molecular weight inhibitor SB431542 (Alk5/4-i), which specifically blocks TGFβ/Activin pathway receptors and does not affect closely related receptors from the bone morphogenetic protein (BMP) pathway or other signal transduction pathways (Ho et al., 2006; Inman et al., 2002; Jazwinska et al., 2007). The mechanism of this selectivity has recently been determined by solving the crystal structure of the mammalian TGFβ type I receptor kinase domain in complex with SB431542 (Ogunjimi et al., 2012). Based on this study, we verified that the key determinant for the selectivity of SB431542, residue S280, as well as all the other gatekeeper residues are conserved in Alk5/4 receptors in zebrafish (supplementary material Fig. S7).

To determine the activity of the SB431542 inhibitor in the heart after cryoinjury, we compared pSmad3 immunostaining between control and inhibitor-treated animals at 14 dpci. We found a noticeable reduction of pSmad3-positive cells within the post-infarct and the myocardium (Fig. 2B,C). We concluded that the application of 10 μM Alk5/4-i markedly suppressed TGFβ/Activin signaling in the heart of adult zebrafish.

To examine the requirement of TGFβ/Activin signaling for heart regeneration, we analyzed the histology of control and Alk5/4-i-treated hearts at different time points after cryoinjury. Acid Fuchsin Orange-G (AFOG) staining of heart sections at 4 dpci revealed a comparable damage of ~20% of the ventricle in control and inhibitor-treated animals with abundant fibrin accumulation (Fig. 3A,B,E,F). At 14 dpci, control hearts formed two domains of the scar: a layer of fibrin along the outer border of the post-infarct, and a network of collagen in the interior of the wound (Fig. 3C). By contrast, the post-infarct of the Alk5/4-i-treated fish failed to deposit a collagenous matrix in the lost myocardium (Fig. 3G). In control hearts at 30 dpci, the fibrotic tissue was largely resolved and was replaced by new muscle tissue, demonstrating substantial cardiac regeneration (Fig. 3D). We found that such a regenerative process was not accomplished after the inhibition of TGFβ/Activin signaling (Fig. 3H). The post-infarct tissue was devoid of muscle and remained surrounded by a layer of fibrin. Moreover, the damaged area conspicuously bulged out from the ventricular circumference, indicating mechanical deformation of the tissue.

To better understand this phenotype, we compared it with another case of defective heart regeneration that occurs upon inhibition of FGF signaling, which has been shown to be required for heart regeneration after partial amputation (Lepilina et al., 2006). As predicted, overexpression of a dominant-negative (dn)

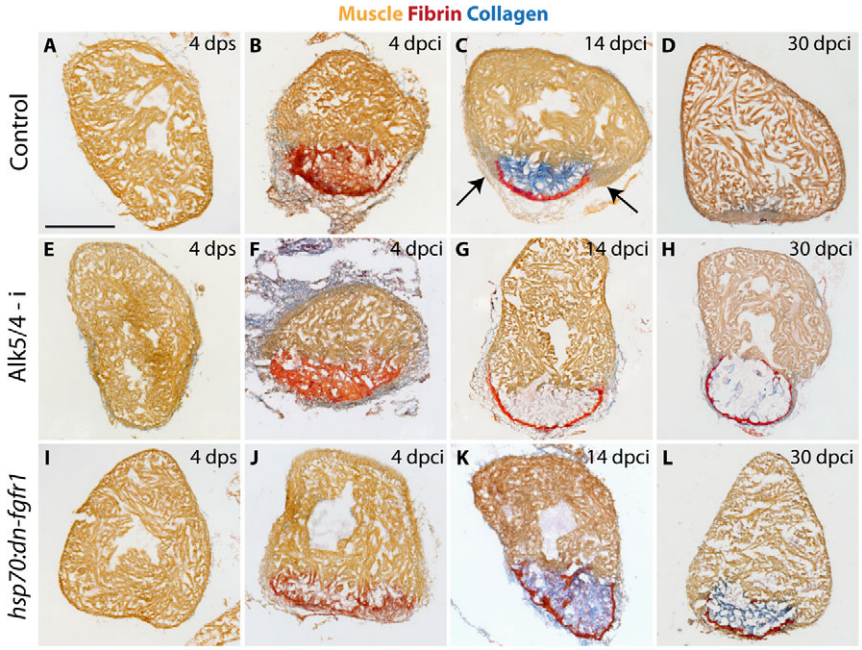

Fig. 3. Inhibition of TGFβ/Activin signaling blocks heart regeneration resulting in the infarct bulging phenotype. Acid Fuchsin Orange-G (AFOG) staining of heart sections visualizes healthy myocardium (orange), fibrin (red) and collagen (blue). (A-D) Control hearts, (E-H) Alk5/4-i-treated hearts, (I-L) hearts of transgenic fish expressing heat shock-inducible *dn-fgfr1*. (**A**,**E**,**I**) Control ventricles after sham operation (4 dps) consist of healthy myocardium. (**B**,**F**,**J**) At 4 dpci, similar infarcts (red) are detected in all experimental groups. (**C**,**G**,**K**) Hearts at 14 dpci. (C) Control hearts contain abundant fibrillar collagen in the injury area. A layer of fibrin (red) covers the margin of the infarct. New myocardium begins to invade the scar tissue (arrows). (G) Exposure to Alk5/4-i suppresses collagen deposition. No myocardial invasion is observed. (K) Inhibition of FGF signaling does not impair collagenous scar formation in comparison to control. (**D**,**H**,**L**) Hearts at 30 dpci. (D) In control hearts, the scar was nearly completely resolved and replaced with new muscle. (H) Alk5/4-i blocked regeneration. The infarct is surrounded by a fibrin layer but it is collagen deficient. The injury area bulges beyond the ventricular circumference. (L) Overexpression of *dn-fgfr1* blocks regeneration, resulting in a collagen-rich scar. No geometrical deformation is associated with the lack of regeneration. Scale bar: 300 μm.

form of the FGF receptor resulted in a lack of cardiac regeneration (Fig. 3I-L). In contrast to the phenotype caused by TGFβ inhibition, the post-infarct of hearts expressing dnFgfr1 contained abundant collagen fibers, indicating excessive scarring. Importantly, the fibrotic infarct did not protrude beyond the ventricular circumference. The phenotypic comparison indicates that TGFβ signaling is required for two processes during heart regeneration: collagen deposition during infarct healing and subsequent cardiac muscle regeneration.

Nonregenerated hearts after Alk5/4-i treatment display cardiac dysfunction

To characterize the nature of the post-infarct tissue of the hearts treated with Alk5/4-I at 30 dpci, we performed immunofluorescence analyses using several cellular and extracellular markers (Chablais et al., 2011). The visualization of Tropomyosin cardiac protein confirmed the absence of myocardial tissue within the protruding post-infarct (supplementary material Fig. S8D,E). Instead, the injury zone was labeled by connective tissue markers, such as the extracellular matrix (ECM) protein Fibronectin and the intermediate filament protein Vimentin. The infarct margin was surrounded by a layer of myofibroblasts/smooth muscle cells that express α-smooth muscle actin (α-SMA). The ECM of the post-infarct was devoid of Tenascin C, a de-adhesive extracellular protein (supplementary material Fig. S8F). By contrast, Tropomyosin-positive myocytes efficiently invaded the post-infarct area in the control hearts. The residual Fibronectin, Tenascin C, α-SMA and Vimentin demarcated the position of cryoinjury (supplementary material Fig. S8A-C). The immunofluorescence analyses demonstrate that the inhibition of TGFβ/Activin signaling impaired the replacement of connective tissue with new cardiac tissue in the post-infarct.

To assess the physiological consequences of this phenotype, we recorded heart conduction with an electrocardiogram (ECG). We have previously shown that cryoinjury results in a prolonged ventricular repolarization, displayed as QT intervals, but that the regenerated hearts at 30 dpci recover their original electrical properties (Chablais et al., 2011). Here, we found that the fish treated with Alk5/4-i for 30 days after cryoinjury developed prolonged QTc values (Fig. 4). Thus, a lack of heart regeneration after the inhibition of TGFβ/Activin signaling alters cardiac electrophysiological properties, indicating heart dysfunction.

TGFβ/Activin-dependent deposition of the transient scar is essential for subsequent regeneration

The phenotype caused by the inhibition of TGFβ/Activin was associated with the absence of a collagen-containing scar and a complete lack of cardiac regeneration (Fig. 3H). Both concomitant defects suggest a correlation between collagenous scar formation observed at 14 dpci and the heart restoration at 30 dpci. To determine whether collagen deposition is beneficial for subsequent cardiac regeneration, we designed a drug-shift experiment. After myocardial infarction, animals were treated with Alk5/4-i during the first 14 days to block collagenous scar formation. Then, the fish were transferred to normal conditions for another period of 14 days to allow regeneration to resume. At the end of the experiment at 28 dpci, heart regeneration and scarring were assayed using AFOG staining (Fig. 5A,C).

Most of the control hearts of this experimental setting displayed advanced regeneration with little scarring (eight hearts per group; Fig. 5A). By contrast, the Alk5/4-i-treated animals failed to restore

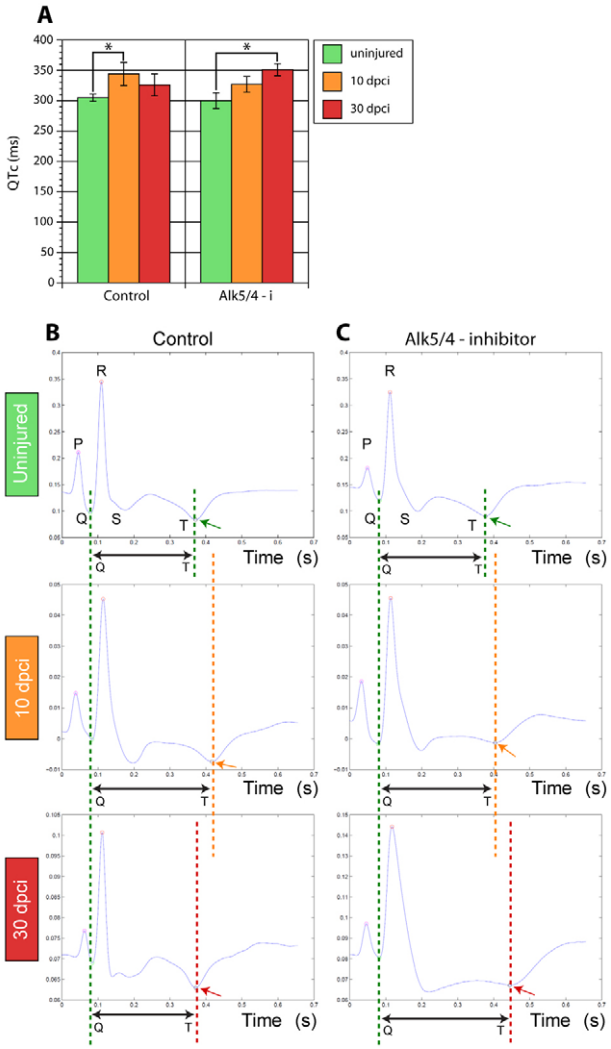

Fig. 4. Electrocardiogram analyses reveal functional defects of nonregenerated hearts after the inhibition of TGFβ/Activin signaling. (**A**) Quantification of QTc interval, an indicator of ventricular action potential, at three different time points after cryoinjury in control and Alk5/4-i-treated fish. In control animals, QTc is significantly prolonged during scar formation at 10 dpci. After regeneration at 30 dpci, the QTc value is similar to that of uninjured hearts, indicating functional recovery. In Alk5/4-i-treated animals, the nonregenerated hearts at 30 dpci display significantly prolonged ventricular action potential (n=6 fish, *P<0.05 compared with uninjured, t-test). Error bars indicate s.e.m. (**B**,**C**) A representative ECG of control (B) and Alk5/4-i-treated (C) animals shortly before the injury at 10 dpci and 30 dpci. Dashed lines indicate the beginning of the QRS waves (Q point) and the end of the ST waves (T point) to compare the QT intervals at different time points. The small colored arrows indicate the end of the ST waves.

the myocardial tissue (among seven animals, four hearts had a bulging infarct, two hearts had impaired regeneration without a significant deformation, and one heart was comparable to the control; Fig. 5C). The post-infarct of these hearts contained collagen fibers, especially around the infarction wall. This demonstrates that the initially blocked deposition of collagen was partially compensated during the 14 days in normal conditions. Despite the resumed regeneration, the cardiac muscle failed to

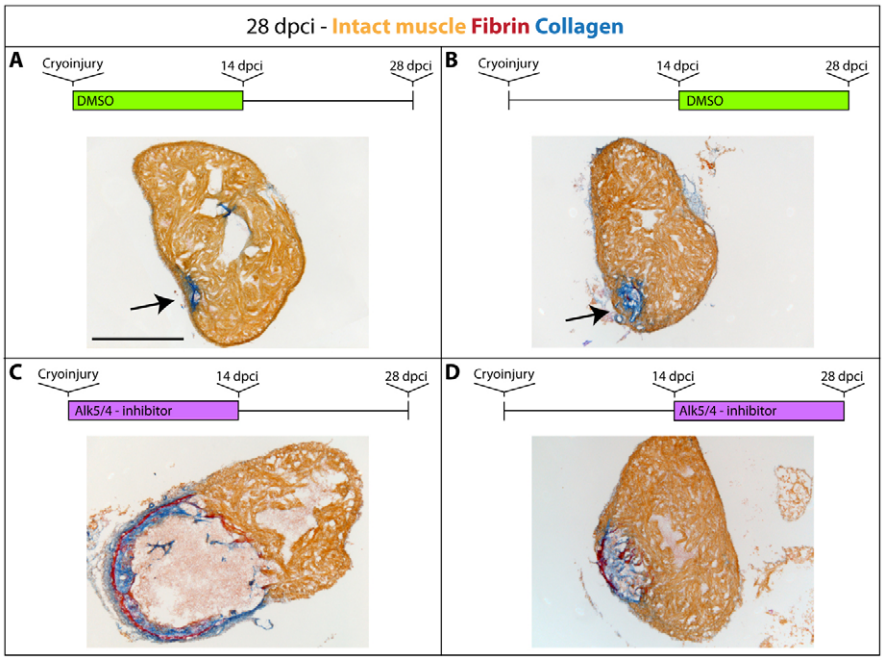

Fig. 5. Transient scar formation is an essential reparative step toward heart regeneration. AFOG staining of zebrafish hearts at 28 dpci after a transient drug treatment during the initial 14 days (A,C) or the final 14 days (B,D) of the experiment. (**A**,**B**) Control (DMSO-treated) hearts display normal regeneration. Only a small area contains collagen fibers (arrow). (**C**) Inhibition of Alk5/4 during the initial phase of scar formation is deleterious, resulting in a complete lack of regeneration. Despite the subsequent 14 days of normal conditions, the post-infarct developed an inflated infarct phenotype. (**D**) Inhibition of Alk5/4 starting at 14 dpci, after the time needed for scar deposition, does not cause architectural deformations of the post-infarct. The injury site contains collagen, but scar replacement with cardiac tissue appears to be impaired in comparison to control (B). Scale bar: 300 μm.

replace the damaged tissue. Thus, the initial suppression of scarring led to irreversibly impaired regeneration. We concluded that TGFβ/Activin-dependent collagen deposition in the subacute phase is essential for subsequent regenerative success.

Alk5/4-i treatment does not promote degradation of pre-existing collagen

Collagen fibers are known to undergo continuous turnover in the healing infarcts (Bowers et al., 2010; Chen and Frangogiannis, 2010). Thus, the stimulatory role of TGFβ for collagen accumulation might occur by either enhancing collagen production and/or decreasing its degradation. To distinguish between these possibilities, we designed an experiment in which the drug treatment was applied after scar formation. For this purpose, the animals were kept in normal conditions for 14 days after cryoinjury to allow collagen deposition. After this time, the fish were transferred to water with Alk5/4-i for the next 14 days, and the amount of scarring was assessed. Histological analysis revealed advanced regeneration with only residual collagen fibers within the post-infarcts of the control hearts (Fig. 5B). By contrast, abundant scar material and regenerative failure were observed after the drug shift (among seven fish, five hearts displayed enhanced scarring without infarct bulging, and two hearts regenerated myocardium with residual scarring comparable to the control; Fig. 5D). The presence of the persisting collagen fibers suggests that the inhibition of Alk5/4 receptors did not enhance degradation of the pre-existing collagenous matrix. We concluded that TGFβ/Activin signaling controls collagen accumulation predominantly by stimulating its synthesis. Moreover, we found no deformation of infarct geometry, indicating a mechanical role of collagen as supporting material in the damaged tissue of the injured heart.

Exposure to Alk5/4-i suppresses the function of fibroblast-like cells in ECM synthesis

The main components of the cardiac ECM include structural proteins such as collagen, adhesive proteins such as fibronectins, and de-adhesive tissue remodeling proteins such as tenascins (Bowers et al., 2010; Corda et al., 2000). We set out to systematically determine the effect of TGFβ/Activin signaling on the expression of these ECM components during the regenerative phase at 14 dpci, when the fibrotic tissue is abundantly detected in the post-infarct. Consistent with our previous observations (Fig. 3G), the accumulation of collagen matrix was strongly impaired in the post-infarcts of Alk5/4-i-treated animals as compared with the controls (Fig. 6A,E,I,L). Moreover, Alk5/4-i treatment resulted in the reduction of Fibronectin, a broadly expressed core matrix component that provides a framework for cell adhesion (Fig. 6C,G). Notably, the tissue remodeling protein Tenascin C (Imanaka-Yoshida et al., 2004), which is normally induced at the infarct-myocardium interface, was completely suppressed after antagonizing Alk5/4 receptors (Fig. 6K,N). Taken together, the deposition of crucial ECM components in the post-infarct zone, including structural, adhesive and de-adhesive proteins, requires TGFβ/Activin signaling.

The source of the ECM in mammalian myocardial infarcts is fibroblasts, myofibroblasts and smooth muscle cells (Camelliti et al., 2005; Dobaczewski et al., 2010b; Porter and Turner, 2009). We aimed to determine whether TGFβ/Activin signaling regulates the ECM content by acting on the recruitment/differentiation of these ECM-producing cells. To visualize the fibroblasts of the infarct we used antibodies against Vimentin, a cytoplasmic intermediate filament-associated protein. The post-infarct of control and Alk5/4-i-treated fish displayed a dense network of Vimentin-positive cells, which was even augmented in the hearts treated with Alk5/4-i (Fig. 6K,N). This accumulation of fibroblasts might represent a compensatory reaction to their reduced activity in the deposition of ECM proteins. To identify myofibroblasts and smooth muscle cells, we used antibodies against α-SMA, a marker of their specific contractile microfilamentous apparatus. In control regenerating hearts, α-SMA specifically labeled the outer border of the post-infarct (Fig. 6D). A similar peripheral rim of α-SMA-positive cells persisted in hearts treated with Alk5/4-i (Fig. 6H). This demonstrates that the inhibition of TGFβ/Activin signaling did not impair the accumulation of Vimentin-positive and α-SMA-positive cells of the fibrotic tissue. Taken together, despite the presence of ECM-producing cells, the synthesis of various ECM components

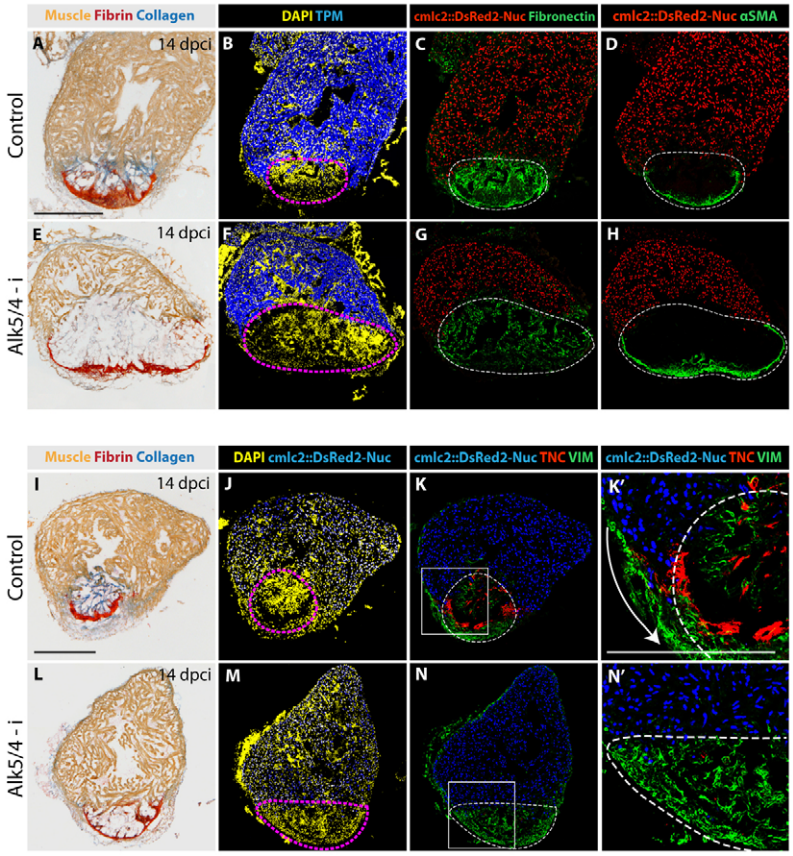

Fig. 6. Inhibition of Alk5/4 impairs the production of ECM proteins in the post-infarct. Analyses of heart sections from transgenic fish expressing nuclear DsRed2-Nuc under the *cmlc2* cardiomyocyte-specific promoter at 14 dpci. Dashed lines represent the injured areas. DsRed2-Nuc is in red (C,D,G,H) or blue (J-K′,M-N′). (A-D,I-K′) Adjacent sections of control hearts. (E-H,L-N′) Adjacent sections of Alk5/4-i-treated hearts. (**A**,**I**) AFOG staining visualizes abundant collagen fibers (blue) at the injury site of control hearts. (**E**,**L**) Inhibition of TGFβ/Activin signaling blocks collagen deposition. (**B**,**F**) The injury site is demarcated by the absence of Tropomyosin protein (blue). The post-infarct is larger in hearts treated with the drug (F) than in control (B). DAPI (yellow) labels all nuclei. (**C**,**G**) Exposure to Alk5/4-i (G) attenuates Fibronectin production (green) in comparison to control (C). (**D**,**H**) α-smooth muscle actin-positive cells (αSMA, green) equally surround the post-infarct border in control and drug-treated hearts. (**J**,**M**) The injury site is demarcated by the absence of *cmlc2::DsRed2-Nuc* (blue). DAPI (yellow) labels all nuclei. (**K**,**K′**,**N**,**N′**) The contra-adhesive matrix protein Tenascin C (TNC, red) is predominantly upregulated at the infarct-myocardium interface in control hearts (K,K′). Treatment with Alk5/4-i completely abolished Tenascin C expression, but increased Vimentin-positive tissue (green; N,N′). (K′,N′) Higher magnifications of the boxed areas in K,N. Arrow (K′) indicates the invasion of new myocardium. Scale bars: 300 μm.

was markedly affected by exposure to Alk5/4-i. We concluded that disruption of TGFβ/Activin signaling results in functionally defective fibroblast-like cells that exhibit impaired ECM deposition.

Epicardial and endocardial cells are important components in heart regeneration in zebrafish (Kikuchi et al., 2011a; Kikuchi et al., 2011b). They induce expression of the RA-synthesizing enzyme Raldh2 (Aldh1a2 – Zebrafish Information Network) to increase production of RA, a cardiogenesis-stimulating factor. To test the role of TGFβ/Activin signaling in the epicardium and the endocardium after myocardial infarction, we immunoassayed Raldh2 in control and Alk5/4-i-treated animals. In uninjured animals, Raldh2 specifically labeled the epicardium (supplementary material Fig. S9). At 14 dpci, Raldh2-positive epicardial cells invaded the injury area and surrounded the damaged myocardium. Consistent with previous studies (Kikuchi et al., 2011b), the expression of Raldh2 was induced in a subset of endocardial cells within the intact myocardium. In comparison with the control animals, inhibition of TGFβ/Activin signaling did not affect the distribution of Raldh2-positive epicardial and endocardial cells (supplementary material Fig. S9B,C). This suggests that the lack of cardiac regeneration in Alk5/4-i-treated fish is not caused by the defective injury responses of epicardium and endocardium.

Inhibition of TGFβ/Activin signaling attenuates cardiomyocyte proliferation

The reparative and regenerative phases of heart regeneration are overlapping, as the deposition of scar tissue is concomitant with the enhanced cell cycle re-entry of cardiomyocytes, which will lead to restoration of the functional cardiac tissue (Chablais et al., 2011). Consistently, closer examination of the control hearts at 14 dpci revealed spreading of myocytes along the border with fibrotic tissue (Fig. 2A and Fig. 6K′). Inhibition of TGFβ signaling impaired this shift of cardiomyocytes into the damaged tissue (Fig. 2B and Fig. 6N′). Notably, the impaired invasion of the myocardium was associated with the suppression of Tenascin C, which is a cell migration-promoting factor at the infarct-myocardium boundary (Imanaka-Yoshida et al., 2004). This observation suggests that TGFβ/Activin signaling is required for the invasion of a new myocardium into the injury area.

To examine the mitogenic role of TGFβ/Activin in regenerating hearts, we assessed cell proliferation with antibodies against Mcm5 (a DNA replication licensing factor) at 14 dpci. To identify nuclei of cardiomyocytes, we used a transgenic strain that expresses nuclear DsRed2 under the control of the *cmlc2* promoter (*cmlc2::DsRed2-Nuc*). In control heart sections with a representative myocardial injury, the proportion of Mcm5-positive cardiomyocytes was 8.6% (Fig. 7A,B). Treatment with Alk5/4-i resulted in a 50% reduction in the number of proliferating cardiomyocytes (Fig. 7B,C). Non-cardiac cell proliferation (Mcm5-positive and DsRed2-negative cells), by contrast, was enhanced by the Alk5/4-i treatment by ~30% (Fig. 7D). This result is consistent with our previous observation of augmented Vimentin-positive tissue in the injury area (Fig. 6K,N). We concluded that the mitogenic role of TGFβ/Activin signaling is tissue dependent: it has a stimulating effect on cardiomyocytes but not on the other cell types of the post-infarct.

The reduced proliferation of myocytes in Alk5/4-i-treated fish can be explained either by the primary requirement of TGFβ/Activin signaling as a mitogenic factor or as the secondary consequence of impaired cell migration and tissue remodeling at the myocardial-infarct boundary. To distinguish between these possibilities, we designed another drug-shift experiment to

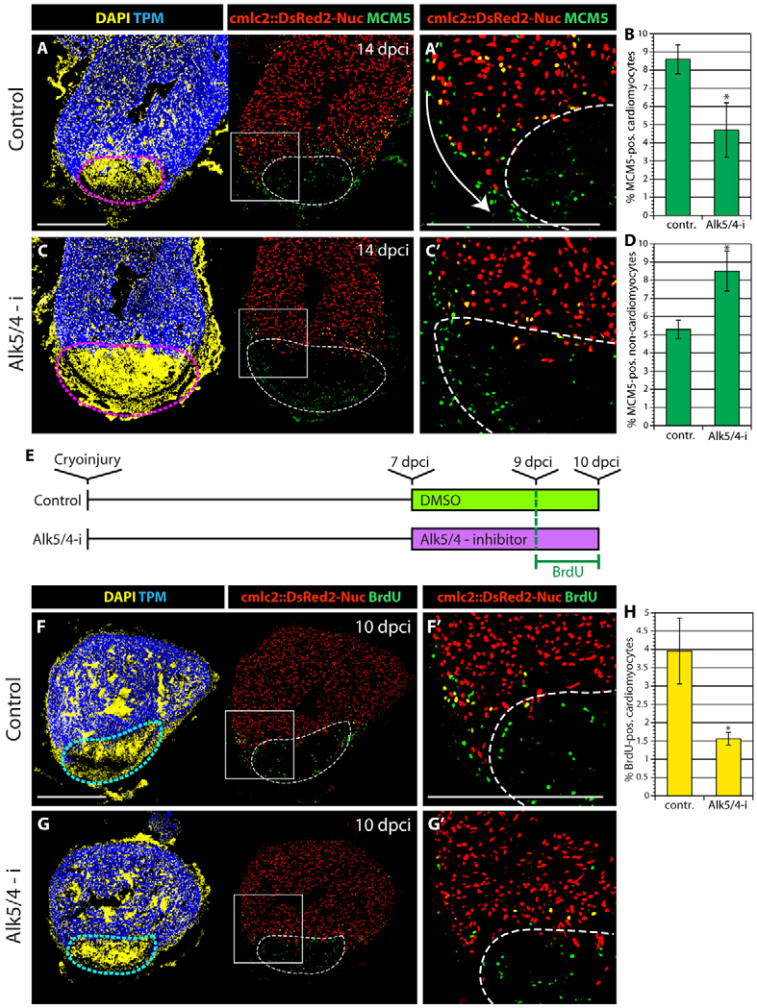

Fig. 7. TGFβ/Activin signaling promotes cardiomyocyte proliferation during heart regeneration. (**A**,**A′**,**C**,**C′**) Heart sections of transgenic *cmlc2::DsRed2-Nuc* (red) fish immunostained for Tropomyosin (blue) and Mcm5 (green) to detect mitotic cells at 14 dpci. DAPI (yellow in the left panels) marks nuclei. Proliferating cardiomyocytes are identified by co-expression of DsRed2 and Mcm5. The post-infarcts are encircled by dashed lines. (A′,C′) Higher magnifications of the boxed areas in A,C. (A,A′) In control hearts, proliferating cardiomyocytes are located in the vicinity of the injury site. Non-cardiac Mcm5-positive cells are distributed predominantly at the post-infarct wall. Arrow (A′) indicates the invasion of new myocardium. (C,C′) Exposure to Alk5/4-i attenuates cardiomyocyte proliferation and expansion. (**B**) The ratio of Mcm5-positive DsRed2-positive nuclei to all DsRed2-positive nuclei demonstrates a reduction of proliferating cardiomyocytes after drug treatment (*n*=10). (**D**) The ratio of Mcm5-positive to DAPI-positive nuclei shows enhanced proliferation of non-cardiac cells after drug treatment (*n*=10). (**E**) Experimental design to demonstrate the immediate effect of Alk5/4-i on cardiomyocyte proliferation. (**F-G′**) Confocal images of hearts from *cmlc::DsRed2-Nuc* (red) transgenic fish. Tropomyosin (blue), DAPI (yellow), BrdU (green). Proliferating cardiomyocytes are identified by the co-expression of DsRed2 and BrdU. Dashed lines indicate the post-infarct. (F′,G′) Higher magnifications of the boxed areas in F,G. (**H**) The ratio of BrdU-positive DsRed2-positive nuclei to all DsRed2-positive nuclei. BrdU incorporation in cardiomyocytes was significantly decreased after Alk5/4-i exposure. Error bars indicate s.e.m.; *n*=10; **P*<0.05, *t*-test. Scale bars: 300 μm.

determine the immediate effects caused by short-term inhibition of Alk5/4 receptors during normally progressing regeneration (Fig. 7E). Transgenic fish after myocardial infarction were first allowed to initiate scar deposition and cardiomyocyte proliferation under normal conditions for the first 7 days, and were then kept in the presence of Alk5/4-i for only 3 days. To identify DNA-replicating cells, the fish were in addition exposed to BrdU for the last 24 hours of the experiment, and cell proliferation was assessed. In sections with scar tissue of control hearts, BrdU labeled ~4% of the cardiomyocytes, which were predominantly located in the vicinity of the injury (Fig. 7F,H). A short-term exposure to Alk5/4-i resulted in a ~70% reduction of BrdU-positive cardiomyocytes (Fig. 7G,H). The rapid reduction of BrdU incorporation suggests that TGFβ/Activin is directly or indirectly required to maintain the proliferative capacity of cardiomyocytes.

To further test the stimulatory role of TGFβ/Activin in cardiac regeneration, we used another injury method that is based on partial amputation of the ventricular apex (Poss et al., 2002). The design of the experiment was the same as that described above, in which the fish after ventricular resection were allowed to initiate regeneration for 7 days under normal conditions, followed by 3 days of Alk5/4-i treatment including BrdU treatment for the final day (supplementary material Figs S10, S11). The pulse exposure to the inhibitor significantly reduced cardiomyocyte proliferation. This demonstrates that the mitogenic role of TGFβ/Activin for cardiomyocytes is independent of the type of heart injury.

DISCUSSION

Heart regeneration following cryoinjury-induced myocardial infarction is remarkably efficient in adult zebrafish (Chablais et al., 2011; Gonzalez-Rosa et al., 2011; Schnabel et al., 2011). The present study identifies the requirement of TGFβ/Activin signaling to coordinate the sequence of diverse cellular events during this process. Our data support a model in which zebrafish heart regeneration can be subdivided into three overlapping phases (Fig. 8). First, myocardial cell death triggers an inflammatory response that is characterized by the infiltration of the infarct with activated leukocytes and fibroblast-like cells, which express TGFβ ligands (Fig. 8A). Second, as the wound becomes cleared of dead cells and matrix debris, the reparative phase begins at ~4 dpci (Fig. 8B). TGFβ/Activin signaling stimulates the recruited fibroblast-like cells to synthesize the collagen-rich ECM. Third, at the onset of scar formation at 7 dpci, the regenerative phase begins (Fig. 8C). While the fibrotic tissue is still maturing, TGFβ/Activin signaling promotes proliferation of cardiomyocytes located in the vicinity of the post-infarct. Tissue remodeling and invasion of new cardiac muscle to replace scar tissue are associated with the TGFβ-dependent expression of Tenascin C, an extracellular protein with contra-adhesive properties. Thus, the regenerative phase is characterized by two opposing processes: scar deposition in the damaged area and scar degradation at the position where new cardiomyocytes invade the post-infarct. It is not known how a balance between both cellular events is achieved. Here, we show

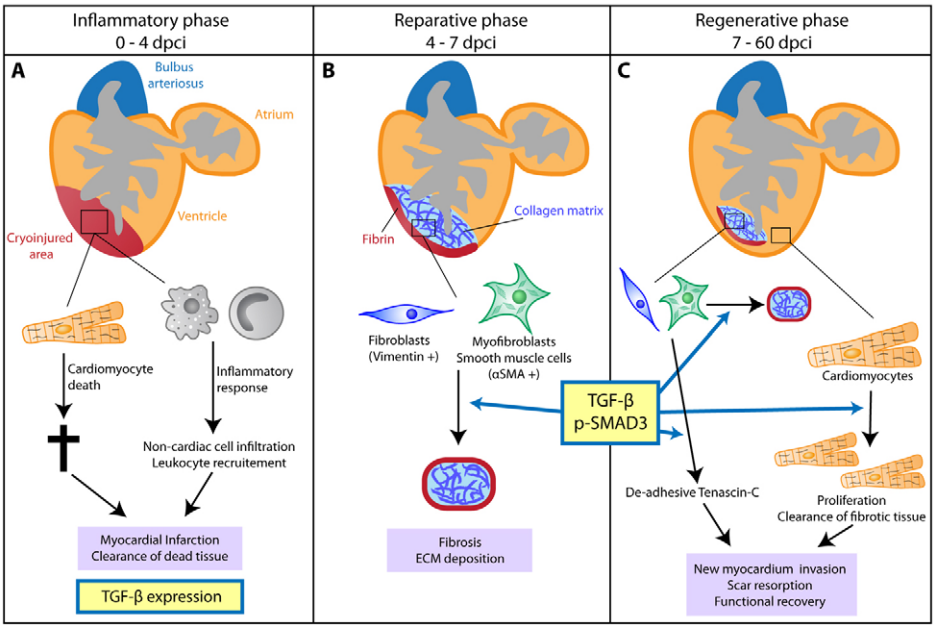

Fig. 8. TGFβ/Activin signaling coordinates the reparative and regenerative phases in response to myocardial infarction. (**A**) Inflammatory phase. In the acute stage after cryoinjury (0-4 dpci), massive death of cardiomyocytes triggers an inflammatory response associated with immune cell infiltration. This response leads to clearance of damaged tissue. (**B**) The reparative phase. During the subacute stage of myocardial infarction (4-7 dpci), non-cardiac cells accumulate at the injury site. TGFβ ligands are transcriptionally induced in the post-infarct. Smad3-mediated TGFβ signaling stimulates infarct healing by enhancing ECM deposition. (**C**) The regenerative phase (7-60 dpci). TGFβ/Activin signaling continues its profibrotic action in the post-infarct, but it also promotes cardiomyocyte proliferation and invasion. The new myocardium progressively replaces the fibrotic tissue, resulting in resolution of the scar and complete cardiac regeneration.

that the equilibrium between the reparative and regenerative responses is coordinated by the TGFβ/Activin signaling pathway. The inhibition of this signaling impairs both collagenous scar formation and cardiomyocyte propagation.

The injury response of the nonregenerative mammalian heart is also described in three phases – inflammation, granulation tissue proliferation and scar maturation – all of which are regulated by multifunctional TGFβ signaling (Dobaczewski et al., 2010b). Although the initial two phases are similar between zebrafish and mammals, in zebrafish the collagenous matrix does not ultimately develop a mature scar but instead undergoes remodeling and is replaced with a new myocardium (Chablais et al., 2011; Gonzalez-Rosa et al., 2011; Schnabel et al., 2011). Thus, the unique feature of the regenerating zebrafish heart is a switch from the deposition to the degradation of fibrotic tissue to allow for the expansion of the new myocardium. Studies in rodents demonstrate that the modulation of TGFβ signaling using pharmacological approaches or gene/protein therapies can reduce fibrosis and deleterious ventricular remodeling (Alegria et al., 2005; Kuwahara et al., 2002; Okada et al., 2005; Tan et al., 2010). Finding the optimal time window for antagonizing TGFβ signaling after myocardial infarction is essential in order to precisely target the pathological processes that occur during the specific phase of heart repair (Leask, 2010).

Downregulation of TGFβ/Activin signaling caused a wide range of cellular phenotypes affecting heart regeneration in zebrafish. Specifically, we identified the following processes to be affected after Alk5/4-i treatment: (1) suppressed collagen accumulation; (2) attenuated Fibronectin deposition; (3) blocked Tenascin C expression at the interface between myocardium and fibroblasts; (4) stimulated fibroblast proliferation; (5) attenuated cardiomyocyte proliferation; and (6) impairment of cardiomyocyte spreading into the post-infarct. These diverse effects demonstrate that TGFβ/Activin signaling can be considered as a molecular link between different responses exerted by various cell subpopulations in the regenerating heart. The comparison between mammalian and zebrafish hearts reveals a common effect on fibroblasts to stimulate their proliferation and ECM protein deposition (Leask, 2007; Dobaczewski et al., 2010a). The most notable difference occurs at the level of the cardiomyocyte response. In mammals, TGFβ promotes pathologic cardiomyocyte hypertrophy (Rosenkranz, 2004), as opposed to the healthy myocyte proliferation observed in zebrafish. These diverse outcomes might be due to either differential intrinsic cardiomyocyte properties or additional environmental factors. Elucidation of these underlying mechanisms will be crucial to understand the differences in regenerative capacities among vertebrates.

One of the important findings of the present study is that the initial transient scar deposition is beneficial for heart regeneration in zebrafish. This discovery is paradoxical to the prevalent concept of ‘scarless regeneration’ in mammalian fetal wound healing, limb regeneration in newts and fin regeneration in teleost fish (Brockes and Kumar, 2008; Palatinus et al., 2010; Poss, 2010). Indeed, in the case of the skin and appendages, the regenerative process can be achieved directly after wound healing without going through a reparative phase of scar formation. We found that such a shortcut is deleterious for the heart as a force-generating contractile organ. Insufficient collagen deposition after Alk5/4 inhibition coincided with the alteration of infarct shape, which was characterized by bulging tissue beyond the ventricular circumference. It is conceivable that a lack of collagen, which normally provides tissue stiffness, affects robustness of the damaged ventricular wall that is challenged to withstand the internal blood pressure (Holmes et al.,

2005). Because the wall tension is proportional to the cavity diameter and inversely proportional to the wall thickness (Laplace's law) (Yin, 1981), the increased ventricular wall stress of the collagen-deficient infarct can lead to biomechanical deformations resulting in an augmented curvature of the infarct. From this physical law, we surmise that transient scar formation is an essential step to maintain ventricular wall stiffness during the subacute regenerative stage. This raises the idea of potential advantages of having a transient scar that can progressively be replaced by new invading functional tissue.

Acknowledgements
We thank V. Zimmermann and M. Kaczorowski for excellent technical assistance and for fish care and M. Celio and N. Panchaud for critical reading of the manuscript. Electrocardiograms were performed in collaboration with G. Rainer and J. Veit.

Funding
This work was supported by the Swiss National Science Foundation [grant number 310030_138062].

Competing interests statement
The authors declare no competing financial interests.

Supplementary material
Supplementary material available online at
http://dev.biologists.org/lookup/suppl/doi:10.1242/dev.078543/-/DC1

References

Alegria, J. R., Herrmann, J., Holmes, D. R., Jr, Lerman, A. and Rihal, C. S. (2005). Myocardial bridging. *Eur. Heart J.* **26**, 1159-1168.
Ausoni, S. and Sartore, S. (2009). From fish to amphibians to mammals: in search of novel strategies to optimize cardiac regeneration. *J. Cell Biol.* **184**, 357-364.
Bowers, S. L., Banerjee, I. and Baudino, T. A. (2010). The extracellular matrix: at the center of it all. *J. Mol. Cell. Cardiol.* **48**, 474-482.
Brockes, J. P. and Kumar, A. (2008). Comparative aspects of animal regeneration. *Annu. Rev. Cell Dev. Biol.* **24**, 525-549.
Camelliti, P., Borg, T. K. and Kohl, P. (2005). Structural and functional characterisation of cardiac fibroblasts. *Cardiovasc. Res.* **65**, 40-51.
Chablais, F. and Jazwinska, A. (2010). IGF signaling between blastema and wound epidermis is required for fin regeneration. *Development* **137**, 871-879.
Chablais, F., Veit, J., Rainer, G. and Jazwinska, A. (2011). The zebrafish heart regenerates after cryoinjury-induced myocardial infarction. *BMC Dev. Biol.* **11**, 21.
Chen, W. and Frangogiannis, N. G. (2010). The role of inflammatory and fibrogenic pathways in heart failure associated with aging. *Heart Fail. Rev.* **15**, 415-422.
Corda, S., Samuel, J. L. and Rappaport, L. (2000). Extracellular matrix and growth factors during heart growth. *Heart Fail. Rev.* **5**, 119-130.
Dobaczewski, M., Chen, W. and Frangogiannis, N. G. (2010a). Transforming growth factor (TGF)-beta signaling in cardiac remodeling. *J. Mol. Cell. Cardiol.* **51**, 600-606.
Dobaczewski, M., Gonzalez-Quesada, C. and Frangogiannis, N. G. (2010b). The extracellular matrix as a modulator of the inflammatory and reparative response following myocardial infarction. *J. Mol. Cell. Cardiol.* **48**, 504-511.
Gonzalez-Rosa, J. M., Martin, V., Peralta, M., Torres, M. and Mercader, N. (2011). Extensive scar formation and regression during heart regeneration after cryoinjury in zebrafish. *Development* **138**, 1663-1674.
Ho, D. M., Chan, J., Bayliss, P. and Whitman, M. (2006). Inhibitor-resistant type I receptors reveal specific requirements for TGF-beta signaling in vivo. *Dev. Biol.* **295**, 730-742.
Holmes, J. W., Borg, T. K. and Covell, J. W. (2005). Structure and mechanics of healing myocardial infarcts. *Annu. Rev. Biomed. Eng.* **7**, 223-253.
Imanaka-Yoshida, K., Hiroe, M. and Yoshida, T. (2004). Interaction between cell and extracellular matrix in heart disease: multiple roles of tenascin-C in tissue remodeling. *Histol. Histopathol.* **19**, 517-525.
Inman, G. J., Nicolas, F. J., Callahan, J. F., Harling, J. D., Gaster, L. M., Reith, A. D., Laping, N. J. and Hill, C. S. (2002). SB-431542 is a potent and specific inhibitor of transforming growth factor-beta superfamily type I activin receptor-like kinase (ALK) receptors ALK4, ALK5, and ALK7. *Mol. Pharmacol.* **62**, 65-74.
Jazwinska, A., Badakov, R. and Keating, M. T. (2007). Activin-betaA signaling is required for zebrafish fin regeneration. *Curr. Biol.* **17**, 1390-1395.
Jopling, C., Sleep, E., Raya, M., Marti, M., Raya, A. and Belmonte, J. C. (2010). Zebrafish heart regeneration occurs by cardiomyocyte dedifferentiation and proliferation. *Nature* **464**, 606-609.
Kikuchi, K., Holdway, J. E., Werdich, A. A., Anderson, R. M., Fang, Y., Egnaczyk, G. F., Evans, T., Macrae, C. A., Stainier, D. Y. and Poss, K. D. (2010). Primary contribution to zebrafish heart regeneration by gata4(+) cardiomyocytes. *Nature* **464**, 601-605.
Kikuchi, K., Gupta, V., Wang, J., Holdway, J. E., Wills, A. A., Fang, Y. and Poss, K. D. (2011a). tcf21+ epicardial cells adopt non-myocardial fates during zebrafish heart development and regeneration. *Development* **138**, 2895-2902.
Kikuchi, K., Holdway, J. E., Major, R. J., Blum, N., Dahn, R. D., Begemann, G. and Poss, K. D. (2011b). Retinoic acid production by endocardium and epicardium is an injury response essential for zebrafish heart regeneration. *Dev. Cell* **20**, 397-404.
Kim, J., Wu, Q., Zhang, Y., Wiens, K. M., Huang, Y., Rubin, N., Shimada, H., Handin, R. I., Chao, M. Y., Tuan, T. L. et al. (2010). PDGF signaling is required for epicardial function and blood vessel formation in regenerating zebrafish hearts. *Proc. Natl. Acad. Sci. USA* **107**, 17206-17210.
Kuwahara, F., Kai, H., Tokuda, K., Kai, M., Takeshita, A., Egashira, K. and Imaizumi, T. (2002). Transforming growth factor-beta function blocking prevents myocardial fibrosis and diastolic dysfunction in pressure-overloaded rats. *Circulation* **106**, 130-135.
Laflamme, M. A. and Murry, C. E. (2011). Heart regeneration. *Nature* **473**, 326-335.
Lawson, N. D. and Weinstein, B. M. (2002). In vivo imaging of embryonic vascular development using transgenic zebrafish. *Dev. Biol.* **248**, 307-318.
Leask, A. (2007). TGFbeta, cardiac fibroblasts, and the fibrotic response. *Cardiovasc. Res.* **74**, 207-212.
Leask, A. (2010). Potential therapeutic targets for cardiac fibrosis: TGFbeta, angiotensin, endothelin, CCN2, and PDGF, partners in fibroblast activation. *Circ. Res.* **106**, 1675-1680.
Lepilina, A., Coon, A. N., Kikuchi, K., Holdway, J. E., Roberts, R. W., Burns, C. G. and Poss, K. D. (2006). A dynamic epicardial injury response supports progenitor cell activity during zebrafish heart regeneration. *Cell* **127**, 607-619.
Lien, C. L., Schebesta, M., Makino, S., Weber, G. J. and Keating, M. T. (2006). Gene expression analysis of zebrafish heart regeneration. *PLoS Biol.* **4**, e260.
Major, R. J. and Poss, K. D. (2007). Zebrafish heart regeneration as a model for cardiac tissue repair. *Drug Discov. Today Dis. Models* **4**, 219-225.
Massague, J. and Gomis, R. R. (2006). The logic of TGFbeta signaling. *FEBS Lett.* **580**, 2811-2820.
Ogunjimi, A. A., Zeqiraj, E., Ceccarelli, D. F., Sicheri, F., Wrana, J. L. and David, L. (2012). Structural basis for specificity of TGFbeta family receptor small molecule inhibitors. *Cell Signal.* **24**, 476-483.
Okada, H., Takemura, G., Kosai, K., Li, Y., Takahashi, T., Esaki, M., Yuge, K., Miyata, S., Maruyama, R., Mikami, A. et al. (2005). Postinfarction gene therapy against transforming growth factor-beta signal modulates infarct tissue dynamics and attenuates left ventricular remodeling and heart failure. *Circulation* **111**, 2430-2437.
Palatinus, J. A., Rhett, J. M. and Gourdie, R. G. (2010). Translational lessons from scarless healing of cutaneous wounds and regenerative repair of the myocardium. *J. Mol. Cell. Cardiol.* **48**, 550-557.
Porter, K. E. and Turner, N. A. (2009). Cardiac fibroblasts: at the heart of myocardial remodeling. *Pharmacol. Ther.* **123**, 255-278.
Poss, K. D. (2010). Advances in understanding tissue regenerative capacity and mechanisms in animals. *Nat. Rev. Genet.* **11**, 710-722.
Poss, K. D., Wilson, L. G. and Keating, M. T. (2002). Heart regeneration in zebrafish. *Science* **298**, 2188-2190.
Rosenkranz, S. (2004). TGF-beta1 and angiotensin networking in cardiac remodeling. *Cardiovasc. Res.* **63**, 423-432.
Rottbauer, W., Saurin, A. J., Lickert, H., Shen, X., Burns, C. G., Wo, Z. G., Kemler, R., Kingston, R., Wu, C. and Fishman, M. (2002). Reptin and pontin antagonistically regulate heart growth in zebrafish embryos. *Cell* **111**, 661-672.
Schnabel, K., Wu, C. C., Kurth, T. and Weidinger, G. (2011). Regeneration of cryoinjury induced necrotic heart lesions in zebrafish is associated with epicardial activation and cardiomyocyte proliferation. *PLoS ONE* **6**, e18503.
Shi, Y. and Massague, J. (2003). Mechanisms of TGF-beta signaling from cell membrane to the nucleus. *Cell* **113**, 685-700.
Singh, B. N., Koyano-Nakagawa, N., Garry, J. P. and Weaver, C. V. (2010). Heart of newt: a recipe for regeneration. *J. Cardiovasc. Transl. Res.* **3**, 397-409.
Tan, S. M., Zhang, Y., Connelly, K. A., Gilbert, R. E. and Kelly, D. J. (2010). Targeted inhibition of activin receptor-like kinase 5 signaling attenuates cardiac dysfunction following myocardial infarction. *Am. J. Physiol. Heart Circ. Physiol.* **298**, H1415-H1425.
Wang, J., Panakova, D., Kikuchi, K., Holdway, J. E., Gemberling, M., Burris, J. S., Singh, S. P., Dickson, A. L., Lin, Y. F., Sabeh, M. K. et al. (2011). The regenerative capacity of zebrafish reverses cardiac failure caused by genetic cardiomyocyte depletion. *Development* **138**, 3421-3430.
Werner, S. and Alzheimer, C. (2006). Roles of activin in tissue repair, fibrosis, and inflammatory disease. *Cytokine Growth Factor Rev.* **17**, 157-171.
Yin, F. C. (1981). Ventricular wall stress. *Circ. Res.* **49**, 829-842.

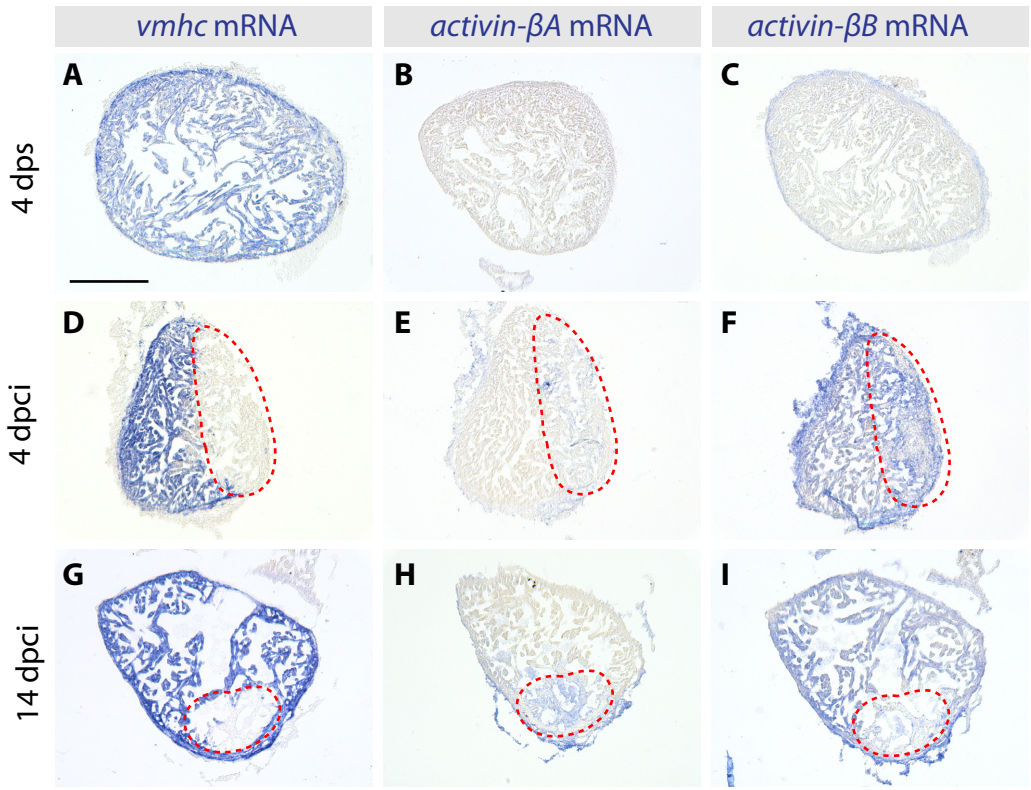
vmhc mRNA
activin-βA mRNA
activin-βB mRNA
4 dps
4 dpci
14 dpci
A
B
C
D
E
F
G
H
I

Table S1. Primers for PCR amplification of genes to generate antisense probes for in situ hybridization

Gene	Gene ID	Forward primer	Reverse primer	Product (bp)
vmhc	NM_001112733	CTGCACTCCCAGAACACAAG	TCAACCAGATCTTGCAGACG	461
tgfb1	NM_182873	TGCAGGATGAGGATGAGGAC	CTGTGTACCCGCAATCCTTG	780
tgfb2	NM_194385	ACGCCAAAGAAGTGCACAAG	CTGTCCGTATCTGTGGAGCG	762
tgfb3	NM_194386	AACCTGAGCACCTCCAGGAC	GCTGCACTTGCAGGATTTG	765
activin-βA	NM_130916	GGGATCCTCCTGCTGCTAAT	AGTGGAAGGACAGCGAGTTG	991
activin-βB	NM_131068	AAGATTCGGGGAGAATGGAC	GTTAGGCACGTCACGTTTGA	1004
alk4	NM_130990	CAACAGCATCAACCTCCAGA	CGGCACCAGGTCATAGTAGG	1000
alk5a	NM_001037683	TCGTGTGCCAAGTGAAGAAG	CATGATCTTGGCCATCACAC	946
alk5b	NM_001115059	GGTGTGTGTGCTGTGTTTCC	ACTGACGGGTCTGACTGGAC	915

To generate antisense probes, the reverse primers were synthesized with addition of the promoter for T3 polymerase.

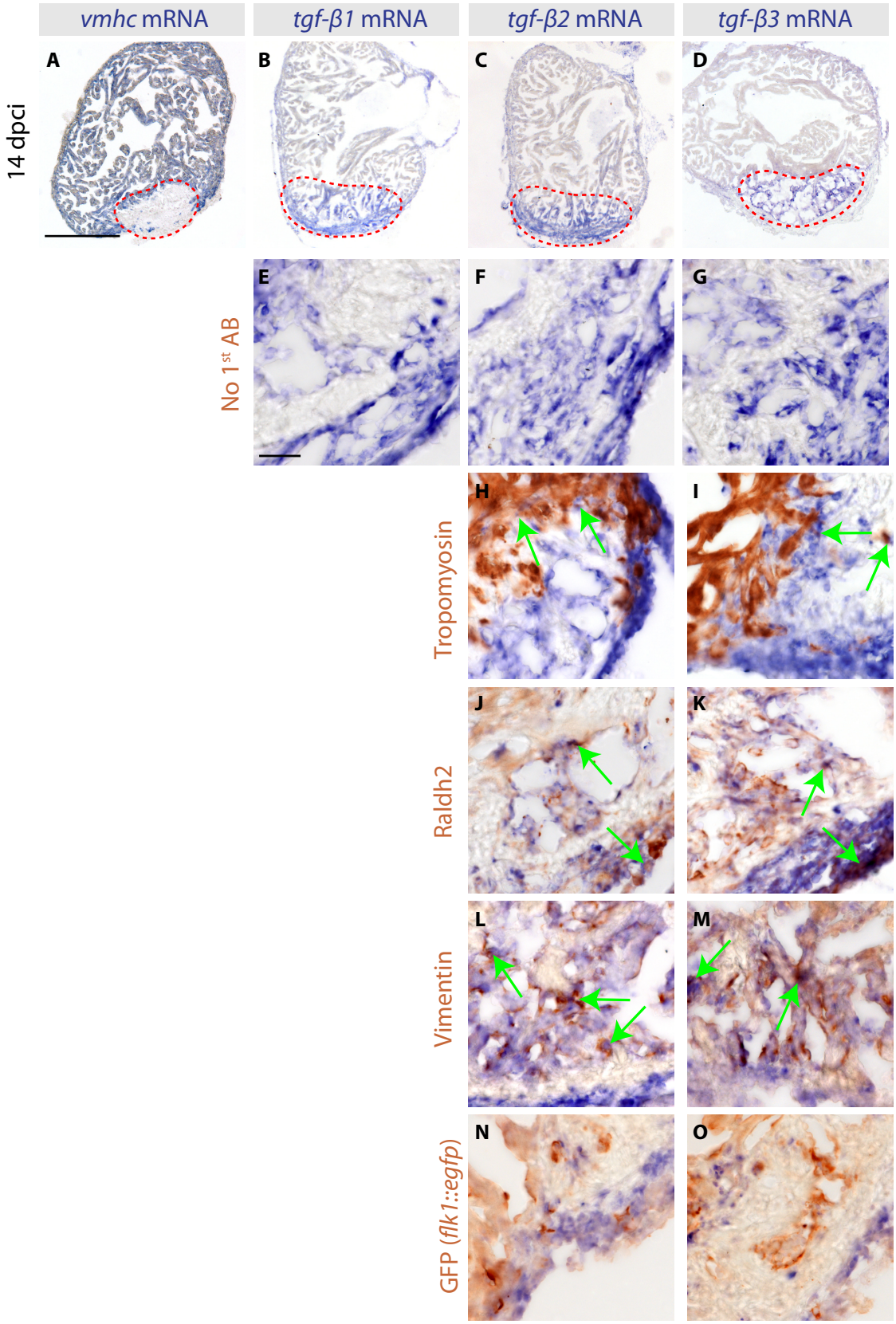
vmhc mRNA
tgf-β1 mRNA
tgf-β2 mRNA
tgf-β3 mRNA
14 dpci
A
B
C
D
No 1st AB
E
F
G
Tropomyosin
H
I
Raldh2
J
K
Vimentin
L
M
GFP (flk1::egfp)
N
O

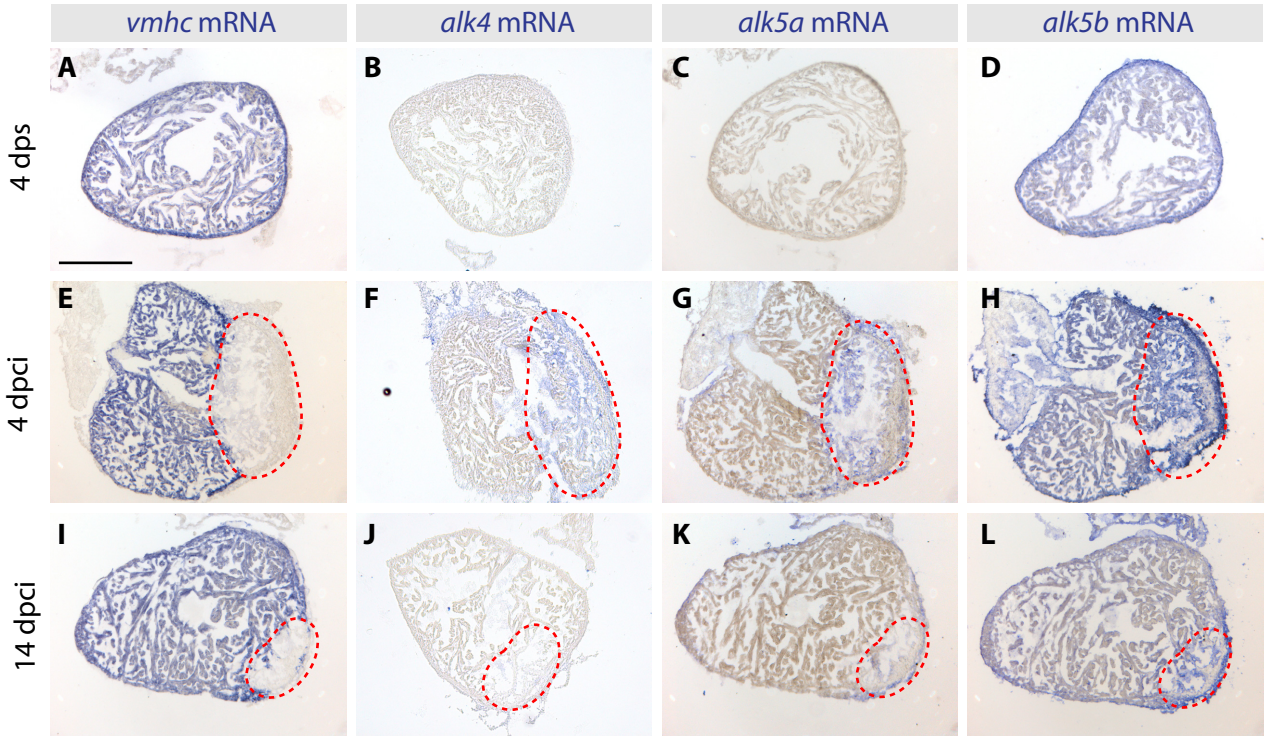
vmhc mRNA
alk4 mRNA
alk5a mRNA
alk5b mRNA
4 dps
4 dpci
14 dpci
A
B
C
D
E
F
G
H
I
J
K
L

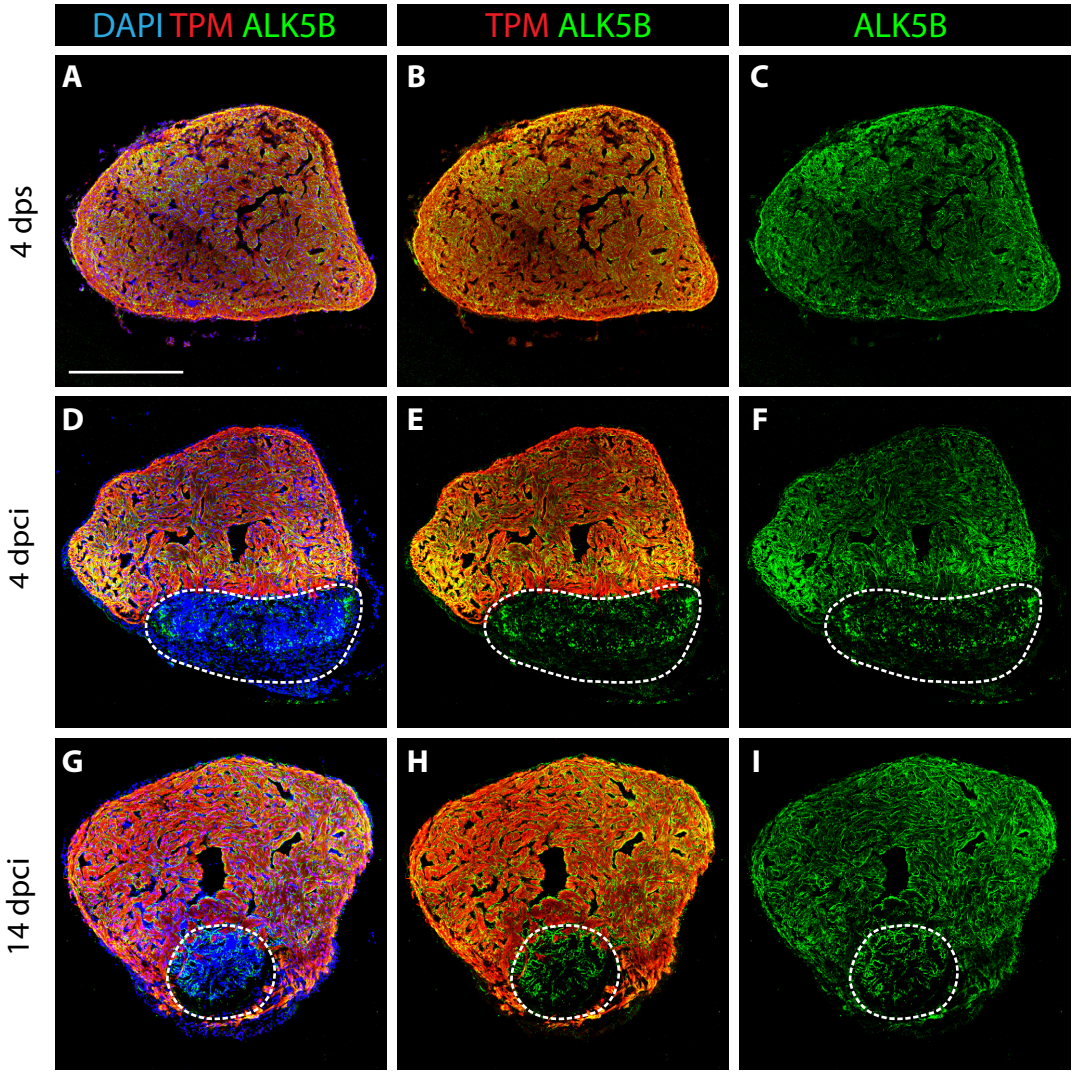
DAPI TPM ALK5B
TPM ALK5B
ALK5B
A
B
C
D
E
F
G
H
I
4 dps
4 dpci
14 dpci

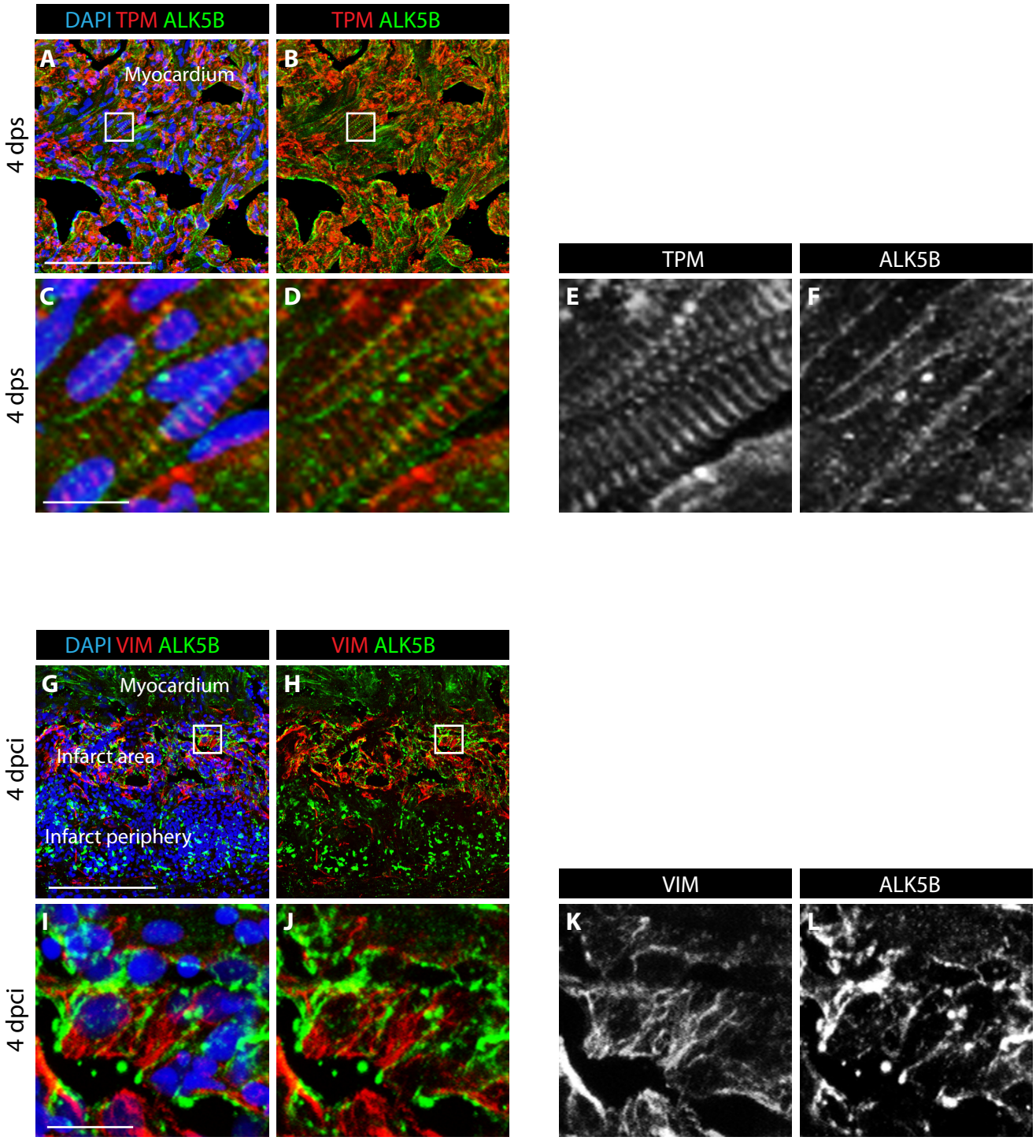
DAPI TPM ALK5B
TPM ALK5B
A
Myocardium
B
4 dps
C
D
4 dps
TPM
ALK5B
E
F
DAPI VIM ALK5B
VIM ALK5B
G
Myocardium
H
Infarct area
Infarct periphery
4 dpci
I
J
4 dpci
VIM
ALK5B
K
L

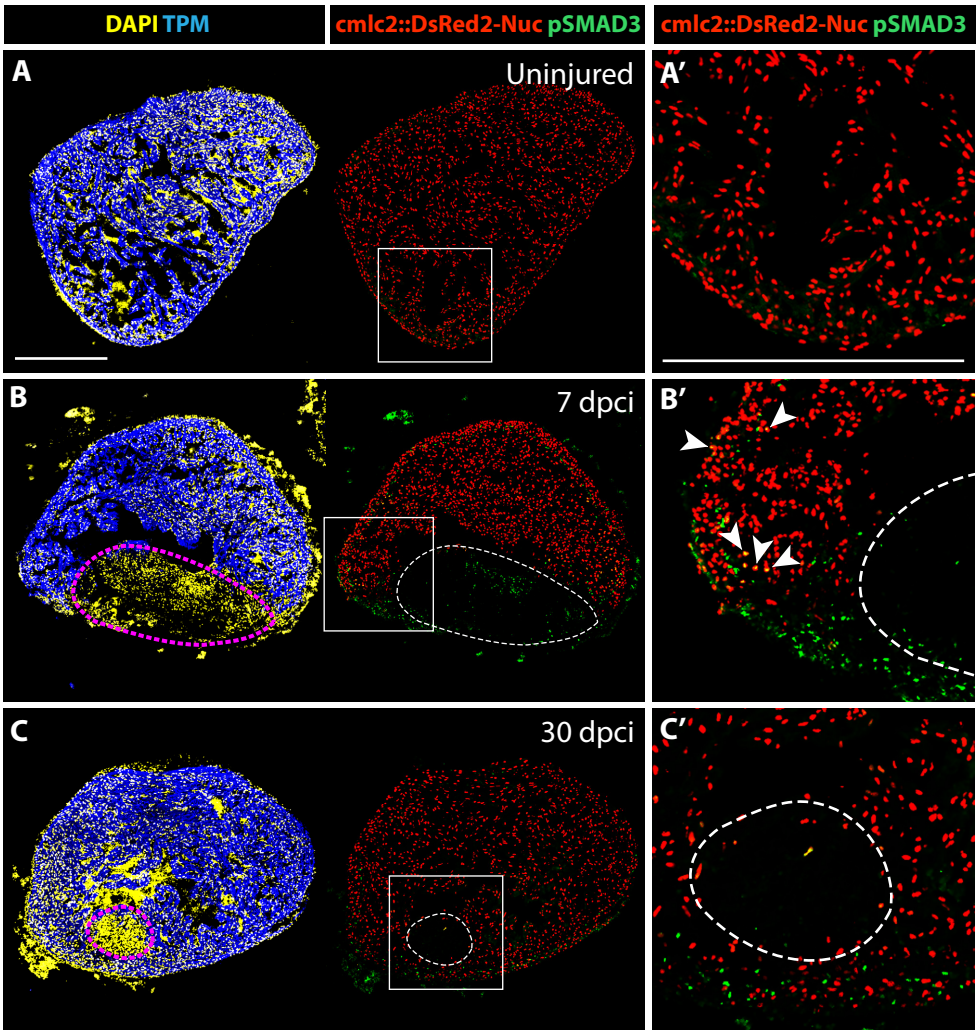
DAPI TPM
cmlc2::DsRed2-Nuc pSMAD3
cmlc2::DsRed2-Nuc pSMAD3
A
Uninjured
A'
B
7 dpci
B'
C
30 dpci
C'

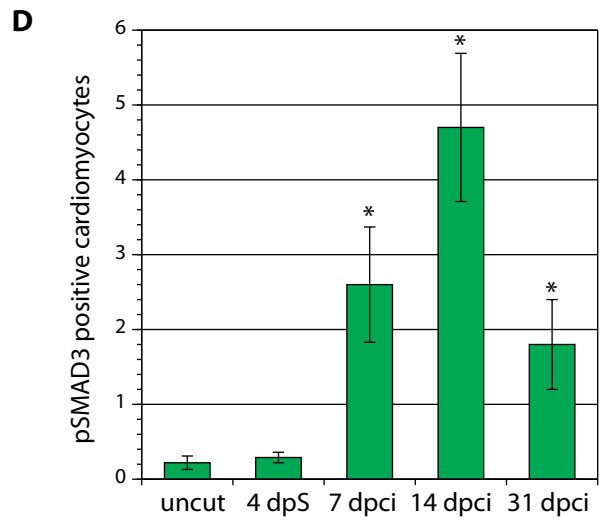
D
pSMAD3 positive cardiomyocytes
0
1
2
3
4
5
6
*
*
*
uncut
4 dpS
7 dpci
14 dpci
31 dpci

A

```
Alk5_Homo          IVLQESIGKGRFGEVWRGKWRGEEVAVKIFSSREERSWFREAEIYQTVML 254
Alk5b_Danio        IILQESIGKGRFGEVWRGRWRGEEVAVKIFSSREERSWFREAEIYQTVML 256
Alk5a_Danio        IILQESIGKGRFGEVWRGRWRGEEVAVKIFSSREERSWFREAEIYQTVML 251
Alk4_Danio         IVLQEIIGKGRFGEVWRGRWRGGDVAVKIFSSREERSWFREAEIYQTIML 256
                   *:*** ************:*** :**********************:**

Alk5_Homo          RHENILGFIAADNKDNGTWTQLWLVSDYHEHGSLFDYLNRYTVTVEGMIK 304
Alk5b_Danio        RHENILGFIAADNKDNGTWTQLWLVSDYHEHGSLFDYLNRYTVTVEGMIK 306
Alk5a_Danio        RHENILGFIAADNKDNGTWTQLWLVSDYHEHGSLFDYLNRYTVTVEGMIK 301
Alk4_Danio         RHENILGFIAADNKDNGTWTQLWLVSDYHEHGSLFDYLNHYSVTIEGMIK 306
                   ************************************:*:**:*****

Alk5_Homo          LALSTASGLAHLHMEIVGTQGKPAIAHRDLKSKNILVKKNGTCCIADLGL 354
Alk5b_Danio        LSLSTASGLAHLHMEIVGTQGKPAIAHRDLKSKNILVKKNGTCCIADLGL 356
Alk5a_Danio        LSLSTASGLAHLHMEIVGTQGKPAIAHRDLKSKNILVKKNGTCCIADLGL 351
Alk4_Danio         LSLSAASGLAHLHMEILGTQGKPGIAHRDLKSKNILVKKNGIFAIADLGL 356
                   *:**:***********:******.*****************  .******

Alk5_Homo          AVRHDSATDTIDIAPNHRVGTKRYMAPEVLDDSINMKHFESFKRADIYAM 404
Alk5b_Danio        AVRHDSATDTIDIAPNHRVGTKRYMAPEVLDDSINMKHFESFKRADIYAM 406
Alk5a_Danio        AVRHDSATDTIDIAPNHRVGTKRYMAPEVLDDSINMRHFESFKRADIYAL 401
Alk4_Danio         AVRHESITDTIDIAPNQRVGTKRYMAPEVLDETINMKHFDSFKCADIYAL 406
                   ****:* *********:***************::***:**:*** *****:

Alk5_Homo          GLVFWEIARRCSIGGIHEDYQLPYYDLVPSDPSVEEMRKVVCEQKLRPNI 454
Alk5b_Danio        GLVFWEIASRCSIGGIHEDYQLPYHDLVQSDPSVEEMRRVVCEQKLRPNI 456
Alk5a_Danio        GLVFWEIARRCSIGGIHEDYQLPYYDLVPSDPSVEDMKRVVCDQKLRPNI 451
Alk4_Danio         GLVYWEIARRCNAGGIHEDYKLPYYDLVPSDPSIEEMRKVVCDQRLRPKW 465
                   ***:**** **. *******:***:*** ****:*:*::***:*:***:

Alk5_Homo          PNRWQSCEALRVMAKIMRECWYANGAARLTALRIKKTLSQL 495
Alk5b_Danio        PNRWQSCEALRVMAKIMRECWYANGAARLTALRIKKTLSQL 497
Alk5a_Danio        PNRWQSCEALRVMAKIMRECWYANGGARLTALRVKKSLSQL 493
Alk4_Danio         PNWWQSYEALRVMGKIMRECWYANGAARLTALRIKKTLSQL 497
                   ** *** ******.***********.*******:**:****
```

B

```
Alk5_Homo          IVLQESIGKGRFGEVWRGKWRGEEVAVKIFSSREERSWFREAEIYQTVML 254
Bmpr1a_Danio       IQTVRMIGKGRYGEVWLGRWRGEKVAVKVFFTREEASWFRETEIYQTVLM 228
Bmpr1b_Danio       IQMVTQIGKGRYGEVWMGRWRGEKVAVKVFFTTEEASWFRETEIYQTVLM 232
                         *****:**** *:****:****:* : ** *****:******::

Alk5_Homo          RHENILGFIAADNKDNGTWTQLWLVSDYHEHGSLFDYLNRYTVTVEGMIK 304
Bmpr1a_Danio       RHENILGFIAADINGTGASTQLYLITDYHENGSLYDYLKFTTLDTQALLR 278
Bmpr1b_Danio       RHDNILGFIAADIKGTGSWTQLYLITDYHENGSLYDYLKCTTLDSRAMLK 282
                   **:********* :..*: ***:*::****:***:***:  *:  ..:::

Alk5_Homo          LALSTASGLAHLHMEIVGTQGKPAIAHRDLKSKNILVKKNGTCCIADLGL 354
Bmpr1a_Danio       LAFSAACGLCHLHTEIYGTQGKPAIAHRDLKSKNILIKKNGTCCIADLGL 328
Bmpr1b_Danio       LAYSSVSGLCHLHTEIFGTQGKPAIAHRDLKSKNILVKRNGACCIADLGL 332
                   ** *:..**.*** ** ********************:*:**:********
```

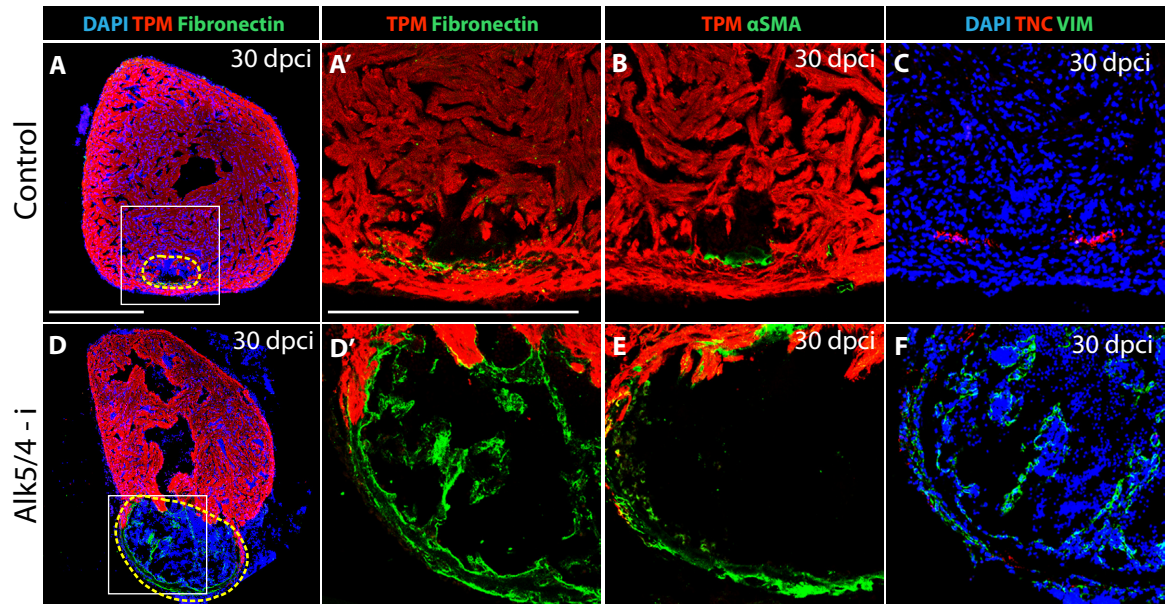
DAPI TPM Fibronectin
TPM Fibronectin
TPM αSMA
DAPI TNC VIM
Control
Alk5/4 - i
A
A'
B
C
D
D'
E
F
30 dpci

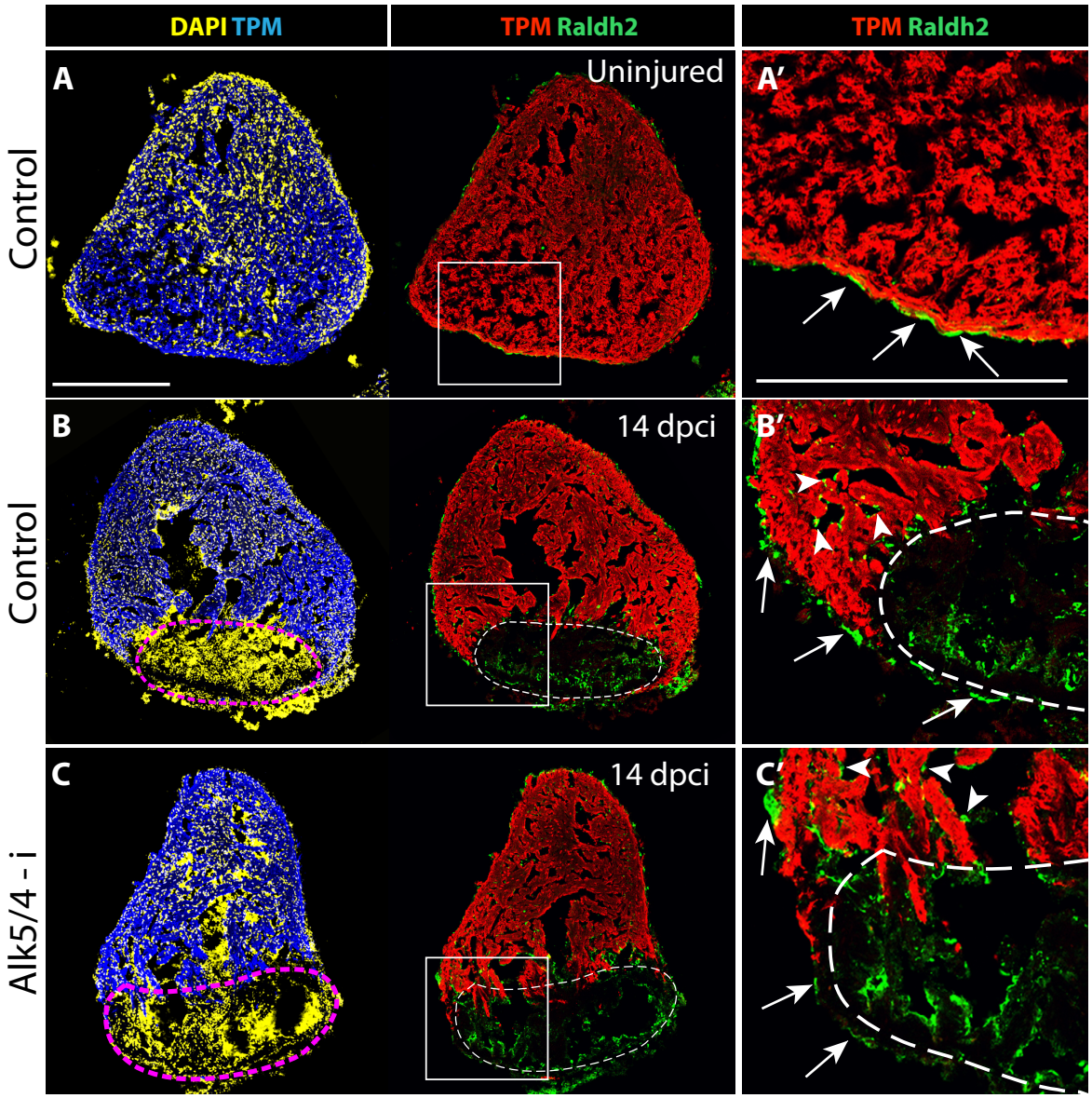
DAPI TPM
TPM Raldh2
TPM Raldh2
Control
Control
Alk5/4 - i
A
Uninjured
A'
B
14 dpci
B'
C
14 dpci
C'

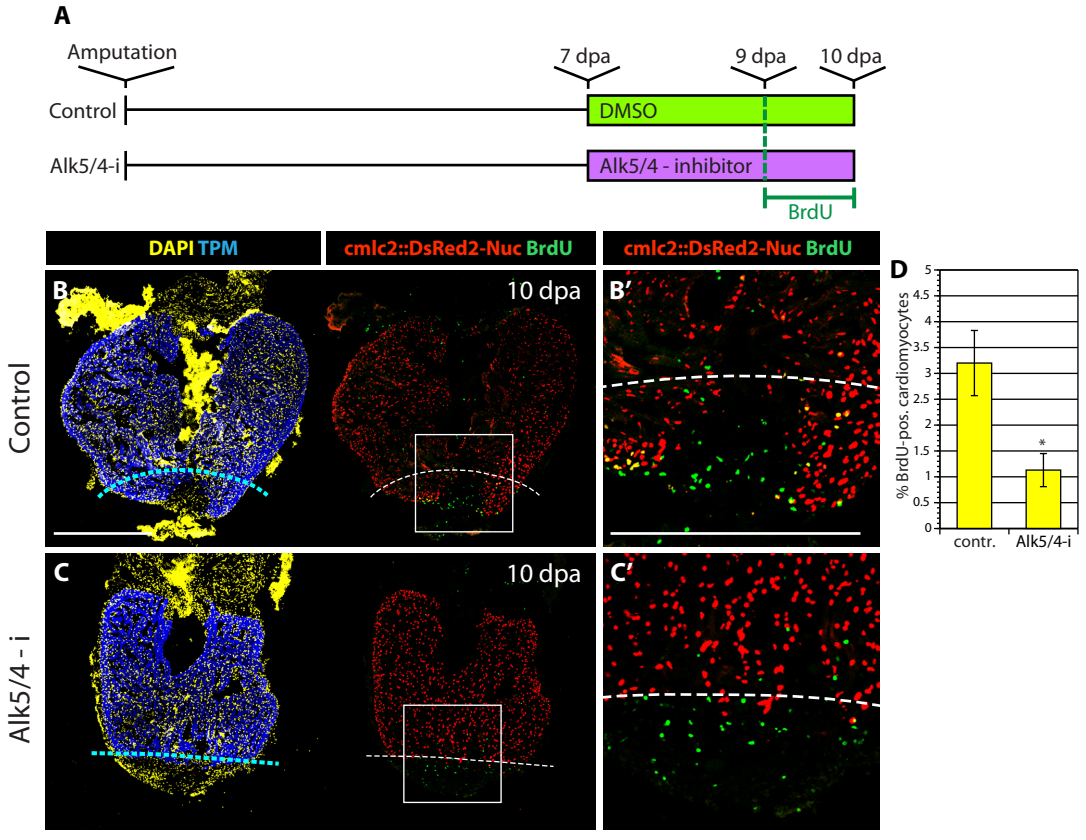
A
Amputation
7 dpa
9 dpa
10 dpa
Control
DMSO
Alk5/4-i
Alk5/4 - inhibitor
BrdU
DAPI TPM
cmlc2::DsRed2-Nuc BrdU
cmlc2::DsRed2-Nuc BrdU
B
10 dpa
B'
C
10 dpa
C'
Control
Alk5/4 - i
D
% BrdU-pos. cardiomyocytes
0
0.5
1
1.5
2
2.5
3
3.5
4
4.5
5
*
contr.
Alk5/4-i

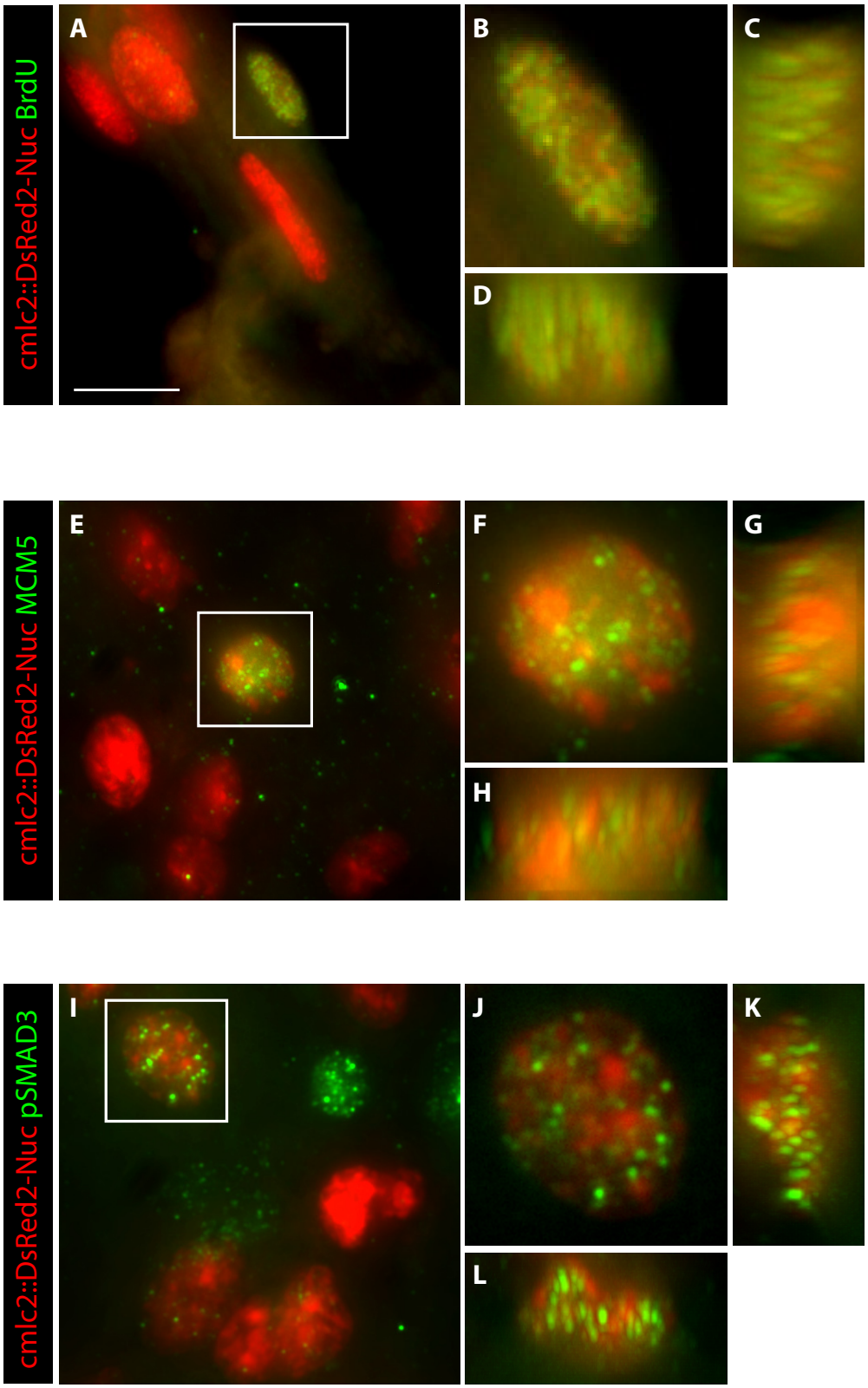
cmlc2::DsRed2-Nuc BrdU
A
B
C
D
cmlc2::DsRed2-Nuc MCM5
E
F
G
H
cmlc2::DsRed2-Nuc pSMAD3
I
J
K
L